AD-A188169

UNCLASSIFIED

NAVAL OCEAN SYSTEMS CENTER, SAN DIEGO, CA
EVALUATION OF ONE- SIDED NUCLEAR MAGNETIC RESONANCE FOR REMOTE DETECTION OF EXPLOSIVES BY: LJ BUNETT, MA FINEMAN

1 OF 2
NOSC TD 1169
UNCLASSIFIED
OCT 1987

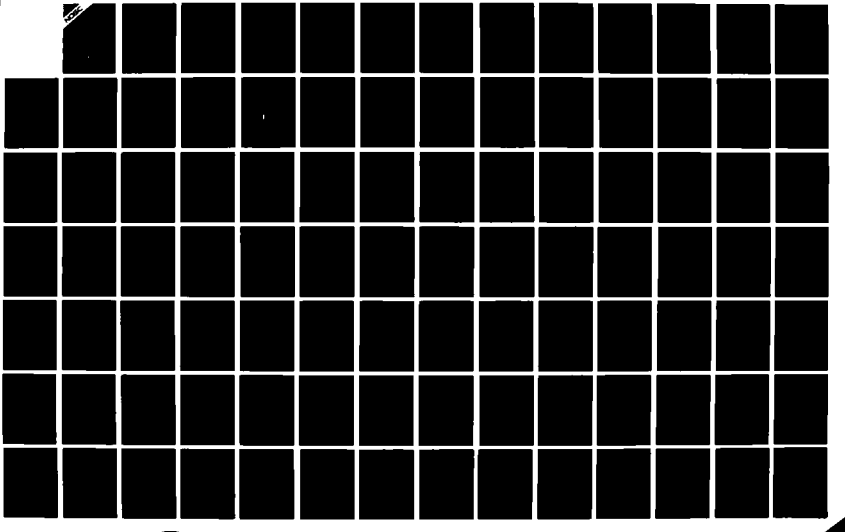

NOSC TD 1169

NAVAL OCEAN SYSTEMS CENTER San Diego, California 92152-5000

Technical Document 1169
October 1987

Evaluation of One-Sided Nuclear Magnetic Resonance for Remote Detection of Explosives

L. J. Burnett
M. A. Fineman
San Diego State University Foundation

NAVAL OCEAN SYSTEMS CENTER

San Diego, California 92152-5000

E. G. SCHWEIZER, CAPT, USN
Commander

R. M. HILLYER
Technical Director

ADMINISTRATIVE INFORMATION

This study was performed for the Electronic Material Sciences Division, Code 56, Naval Ocean Systems Center, by the San Diego State University Foundation.

Released under the authority of
A.K. Nedoluha, Head
Electronic Material Sciences Division

JG

UNCLASSIFIED
SECURITY CLASSIFICATION OF THIS PAGE

REPORT DOCUMENTATION PAGE

1a REPORT SECURITY CLASSIFICATION UNCLASSIFIED	1b RESTRICTIVE MARKINGS
2a SECURITY CLASSIFICATION AUTHORITY	3 DISTRIBUTION/AVAILABILITY OF REPORT Approved for public release; distribution is unlimited.
2b DECLASSIFICATION/DOWNGRADING SCHEDULE	
4 PERFORMING ORGANIZATION REPORT NUMBER(S)	5 MONITORING ORGANIZATION REPORT NUMBER(S) NOSC TD 1169
6a NAME OF PERFORMING ORGANIZATION San Diego State University Foundation 6b OFFICE SYMBOL (if applicable) SDSU	7a NAME OF MONITORING ORGANIZATION Naval Ocean Systems Center
6c ADDRESS (City, State and ZIP Code) 5300 Campanile Drive San Diego, CA 92182	7b ADDRESS (City, State and ZIP Code) San Diego, CA 92152-5000
8a NAME OF FUNDING/SPONSORING ORGANIZATION Naval Ocean Systems Center 8b OFFICE SYMBOL (if applicable) Code 56	9 PROCUREMENT INSTRUMENT IDENTIFICATION NUMBER
8c ADDRESS (City, State and ZIP Code) San Diego, CA 92152-5000	10 SOURCE OF FUNDING NUMBERS PROGRAM ELEMENT NO: 62762N; PROJECT NO: X62588; TASK NO: EE90; AGENCY ACCESSION NO: DN307 379

11 TITLE (Include Security Classification)

Evaluation of One-Sided Nuclear Magnetic Resonance for Remote Detection of Explosives

12 PERSONAL AUTHOR(S)

L.J. Burnett and M.A. Fineman, SDSU Foundation

13a TYPE OF REPORT	13b TIME COVERED	14 DATE OF REPORT (Year, Month, Day)	15 PAGE COUNT
Final	FROM _____ TO _____	October 1987	112

16 SUPPLEMENTARY NOTATION

17 COSATI CODES			18 SUBJECT TERMS (Continue on reverse if necessary and identify by block number)
FIELD	GROUP	SUB-GROUP	Nuclear magnetic resonance Explosives detection

19 ABSTRACT (Continue on reverse if necessary and identify by block number)

This study defines the problem of nuclear magnetic resonance (NMR) remote detection of explosives, gathers available data on the materials of interest, defines a figure-of-merit suitable for comparing alternative instrument configurations, and uses the figure-of-merit to identify one or more remote detection NMR systems with the potential to contribute to the solution of the detection problem.

20 DISTRIBUTION/AVAILABILITY OF ABSTRACT	21 ABSTRACT SECURITY CLASSIFICATION
☐ UNCLASSIFIED/UNLIMITED ☒ SAME AS RPT ☐ DTIC USERS	UNCLASSIFIED
22a NAME OF RESPONSIBLE INDIVIDUAL A.K. Nedoluha, COTR	22b TELEPHONE (Include Area Code) (619)225-6591
	22c OFFICE SYMBOL Code 56

DD FORM 1473, 84 JAN

83 APR EDITION MAY BE USED UNTIL EXHAUSTED
ALL OTHER EDITIONS ARE OBSOLETE

UNCLASSIFIED
SECURITY CLASSIFICATION OF THIS PAGE

EXECUTIVE SUMMARY

This program was initiated to investigate the potential of nuclear magnetic resonance (NMR) for remote detection. Remote regions accessible from only one side and the remote detection of explosives were topics of particular interest.

The program involved the following seven specific tasks and subtasks: (1) to identify the compounds of interest, both benign and explosive; (2) to locate and catalog available data on the compounds of interest; (3) to review current remote NMR technology; (4) to identify alternative remote NMR systems; (5) to define a figure-of-merit suitable for comparing the alternative NMR systems; (6) to use the figure-of-merit to identify the most promising of the alternative systems; and (7) to predict the performance of the chosen system. Each of these tasks was completed successfully.

The present state of remote NMR technology and the principal conclusions of this study are outlined below.

* Remote detection by single-sided NMR is feasible. Present systems produce low static fields (less than 500 Gauss) at modest penetration depths (10 cm).

* The most promising advanced remote NMR system configuration utilizes an Inside-Out Helmholtz pair of current loops to produce the static magnetic field and a semitoroid coil to produce the rf field.

* The advanced NMR remote detection system will employ superconducting coils to produce magnetic fields of 1,000 Gauss or more at penetration depths in excess of 20 cm. New cryogenic materials and fabrication techniques should eliminate many of the difficulties previously associated with the use of superconducting technology.

* Available data indicate that NMR remote detection of the following explosives is possible: Compound B, Compound C-4, PETN, RDX, TATB, and TNT. Data on the NMR properties of explosives are sparse.

* It may be possible to define a unique signature for many explosive compounds by taking advantage of hydrogen-nitrogen nuclear interactions.

Additional laboratory data and analyses are required to determine the range of applicability of this technology and to address the practical problems associated with its implementation.

TABLE OF CONTENTS

TABLE OF CONTENTS (Continued)

TABLE OF CONTENTS (Continued)

LIST OF FIGURES

LIST OF FIGURES (Continued)

LIST OF FIGURES (Continued)

LIST OF TABLES

I. INTRODUCTION

The reliable detection of explosives in remote or inaccessible regions poses difficult technical problems. The purpose of the present program is to explore and evaluate the potential of one-sided, or single-sided, nuclear magnetic resonance (NMR) for the remote detection of explosives.

NMR utilizes nonionizing radiation to manipulate the weak magnetism of atomic nuclei. The non-ionizing radiation, a combination of AC and DC magnetic fields, is applied to the region to be inspected. Shortly thereafter, a radio frequency signal is received from the nuclei. The characteristics of this signal are related to the chemical properties of the material containing the nuclei.

This study was limited exclusively to NMR of hydrogen nuclei. Hydrogen nuclei give a strong NMR response and are abundant in most of the materials of interest. Hydrogen is, without doubt, the only nucleus likely to provide an NMR signal strong enough for the detection applications considered.

In addition, under certain conditions, the hydrogen NMR signals of many explosive compounds possess an almost-unique signature. This signature, based upon differences in NMR parameters called relaxation times, provides the foundation for a simple and direct detection method.

NMR detection systems are capable of performing well in a field environment. As an example, an NMR system to detect narcotics in the mails was recently field tested at the Worldway Postal Center in Los Angeles (1). The NMR system was designed to respond to the relaxation signature of cocaine. A total of 3,350 letters were examined. Seven alarm responses were recorded; two were false alarms, and five were due to letters containing cocaine.

An important reason for the success of this field test was that the NMR system was not forced to encounter large quantities of benign and potentially-interfering materials (other than paper) during the inspection process. Since the volume of the inspection region in remote detection NMR is limited, it should be noted that the NMR systems discussed in this report may display similarly favorable inspection properties, even in complex detection situations.

This study extends previous work in remote detection NMR, principally Single-Sided NMR and Inside-Out NMR. Previous implementations of Single-Sided NMR (2,3,4) have employed iron-yoke electromagnets to produce the required region of remote field. These systems were developed to measure moisture levels in subsurface soils and in structural concrete.

Inside-Out NMR (5,6,7) utilizes opposed magnets to produce a toroidal field geometry. This type of remote NMR system was developed for geophysical exploration, i.e., as a borehole logging tool to evaluate subsurface rock formations and hydrocarbon deposits.

The principal objectives of this study were to define the problem of NMR remote detection of explosives; gather available data on the materials of interest, both benign and explosive; define a figure-of-merit suitable for comparing alternative instrument configurations; and utilize the figure-of-merit to identify one or more remote detection NMR systems with the potential to contribute to the solution of the detection problem. All of the principal objectives of this study were achieved.

This report is organized along the lines of the study itself, beginning in Chapter II with a brief presentation of NMR fundamentals. A discussion of the NMR properties and molecular structures of the materials of interest, which include both explosive and benign substances, follows in Chapter III.

A discussion of system components for remote NMR is presented in Chapter IV. A review of the possible combinations of these components leads quite naturally to several potential systems. These systems are discussed and evaluated in Chapter V.

The most promising configuration for a single-sided NMR system is presented in Chapter VI. The system signal-to-noise ratio is calculated and practical considerations are discussed. Conclusions and recommendations, which are quite positive concerning the potential of single-sided NMR for explosives detection, are presented in Chapter VII.

II. NMR FUNDAMENTALS

A. Introduction

The phenomenon of nuclear magnetic resonance (NMR) arises from the fact that the nuclei of many atoms possess both magnetic moments and angular momenta (8,9). In particular, hydrogen nuclei, or protons, which are found in most materials, exhibit magnetic properties especially suitable for the observation of nuclear magnetic resonance.

When subjected to a static magnetic field, the hydrogen nuclei align at an angle to the field, pointing either with the field or against it, and then precess about the field at a frequency called the Larmor frequency. The static magnetic field is often called the Ho field. The Larmor frequency is proportional to the strength of the applied field, and for an applied field of 1,000 Gauss (about 2,000 times the strength of the earth's magnetic field) the Larmor frequency is 4.26 Megahertz (MHz). For readily-attainable magnetic fields, and for most nuclei, Larmor frequencies fall within the radio-frequency (or rf) range from about 0.3 - 300 MHz.

Nuclear magnetic resonance arises when an oscillating, or rf, magnetic field is applied to the precessing nuclei. This rf field is called the Hl field, and it is applied in a direction perpendicular to the Ho field.

If the Hl field oscillates at the Larmor frequency, then some of the nuclei that were originally aligned with the static field will realign against it. The net effect is the resonant absorption of a very small amount of energy from the rf field, and this resonant absorption is called nuclear magnetic resonance (NMR).

B. Pulse NMR

A common way to observe a nuclear magnetic resonance signal involves placing a sample, which contains the nuclei of interest, into a static magnetic field and then applying a short, intense pulse of rf field at the Larmor frequency. The technique is called pulse NMR (10).

Following the rf pulse, the nuclei precess in phase. If a coil is located nearby, this in-phase precession of nuclear magnets induces a transient voltage across it. This transient voltage is the NMR signal, which is called the free induction decay (FID). A sketch of an NMR FID is shown in Figure II-1. The adjacent coil, often called the sample coil, is generally wound around the sample to ensure efficient coupling. The sample coil is also used, in many configurations, to apply the rf pulse.

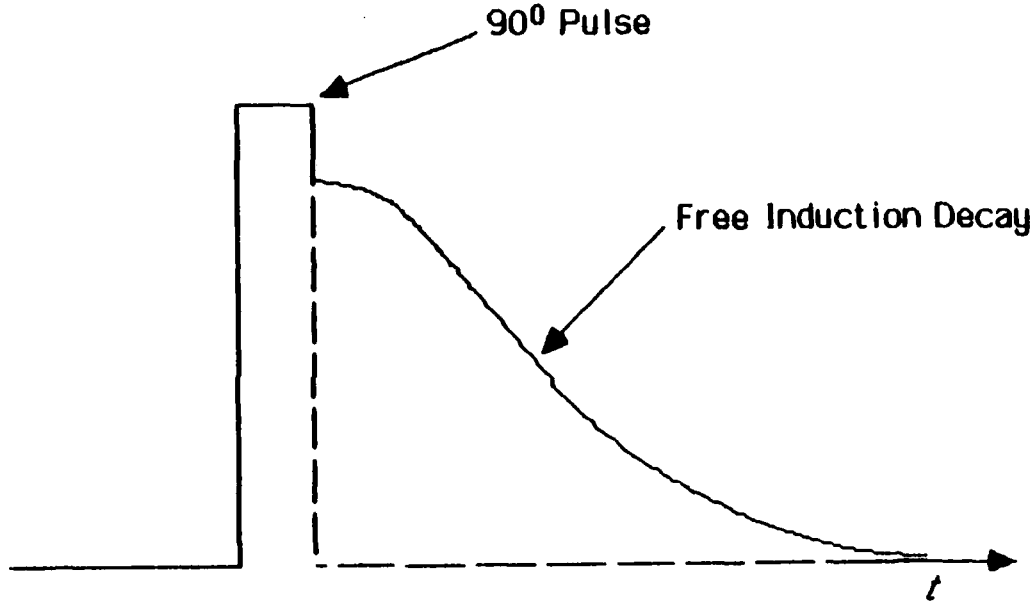

Sketch of an NMR Free Induction Decay

Figure II-1

The magnitude of the FID signal following the rf pulse depends upon the duration of the pulse. A pulse of a certain length, called a 90-degree pulse, produces a maximum in the transient in-phase precession of the nuclear moments and, hence, a maximum FID signal following the pulse. In fact, the effect of a 90-degree pulse is to tip the nuclear magnetization away from the direction of the Ho field by 90 degrees.

A pulse of twice the length, called a 180-degree pulse, produces a minimum in the transient nuclear precession and, under ideal conditions, results in a zero FID response. In a fashion similar to the 90-degree pulse, the effect of a 180-degree pulse is to tip the nuclear magnetization away from the direction of the Ho field by 180 degrees.

Short, intense rf fields impressed upon the nuclear spin system produce effects that are difficult to characterize in a brief discussion. For an in-depth treatment of the subject, comprehensive references are readily available (10,11).

C. Laboratory Pulse NMR Systems

A block diagram of a typical, laboratory-type pulse NMR system is shown in Figure II-2. The magnet applies a static magnetic field to the sample, while the radio frequency transmitter generates the rf pulses. The rf pulses are applied to the sample through the coupling network and sample coil, which are also used to receive the NMR free induction decay (FID) signal.

The NMR receiver, tuned to the Larmor frequency, amplifies the weak FID signal prior to processing and display. The controller is responsible for circuit timing; it controls the duration of the pulses, the number of pulses in the test sequence, the timing of data acquisition windows, and other similar tasks.

D. Remote Pulse NMR Systems

The block diagram of an NMR system for remote detection is very similar to that of the laboratory system described above. However, since access to the sample is restricted, remote NMR imposes special requirements on both the magnet system and the sample coil.

There are three problems in implementing single-sided remote NMR: (1) a magnet geometry must be defined that will produce a homogeneous DC field in a remote region where access is limited to only one side; (2) an rf field must be produced within this remote region of DC field; and (3) the direction of the rf field must be perpendicular to the direction of the DC field. Practical solutions to each of three problems will result in a useable remote detection NMR system.

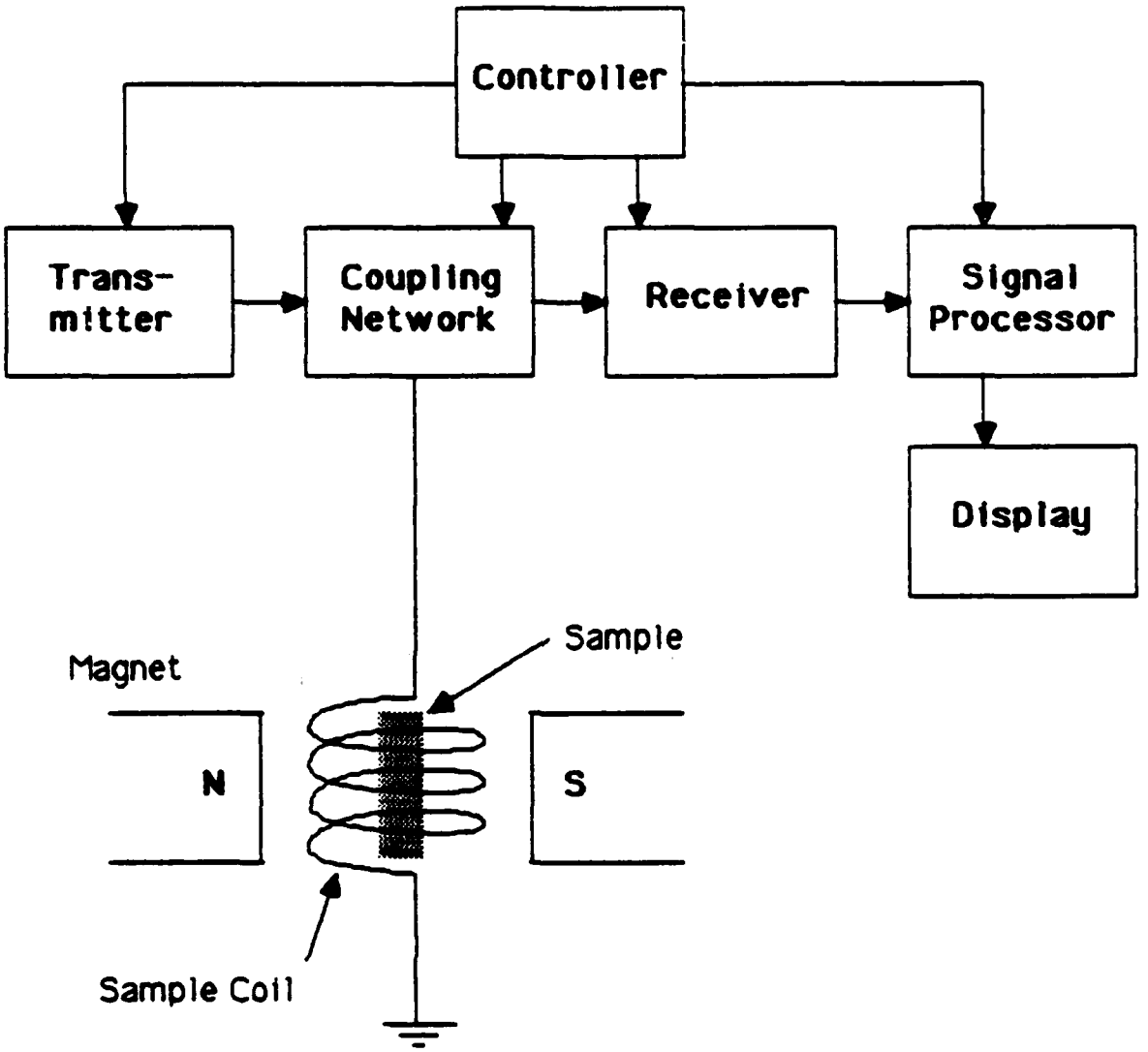

Block Diagram of a

Pulse NMR System

Figure II-2

E. Spin-Lattice Relaxation

In pulse NMR, if the rf pulse is of the proper duration and intensity, the nuclei absorb energy during the pulse and, therefore, at the end of the pulse, are out of equilibrium with their surroundings. The characteristic time for the nuclei to return to equilibrium is called the spin-lattice relaxation time, T1. For protons in common substances in typical magnetic fields, T1 ranges from hundreds of microseconds to hundreds of seconds.

Spin-lattice relaxation times are commonly measured in the laboratory with the (180 - tau - 90) pulse sequence shown in Figure II-3. First, a 180-degree, or "pi", pulse is applied to the sample. The nuclear magnetization is tipped by 180 degrees, from its equilibrium value Mo to -Mo. Following the pulse the nuclear magnetization begins to return toward equilibrium. After a time tau (the pulse delay time) has elapsed, a 90-degree pulse is applied. The magnitude of the FID following this pulse is proportional to the state of the magnetization at time tau. The initial magnitude of the FID is recorded, and the experiment is repeated for a number of different pulse delay times. A plot of the FID magnitude versus tau provides the characteristic time for the return of the nuclear magnetization to equilibrium. This characteristic time is T1, the spin-lattice relaxation time.

Relaxation times in NMR are influenced strongly by molecular motions which alter the angles and distances between nuclei. In many compounds, the rate and nature of molecular motion completely determines the spin-lattice relaxation time T1. These effects are discussed in Chapter III, following a discussion of the spin-spin relaxation time and the NMR solid echo.

F. Spin-Spin Relaxation

One effect of the rf pulse is to align the nuclear magnets and, at the end of a 90-degree pulse, all the nuclei are precessing in phase. They do not precess in phase forever, though. Because neighboring nuclei are magnetic, each nucleus is found in a magnetic field that is the sum of the externally-applied field and a local field due to the presence of neighboring nuclei. Hence, there is a spectrum of precession frequencies for nuclei within the sample.

If the spectrum of precession frequencies is narrow, then all the nuclei precess at essentially the same frequency. Following an rf pulse, they remain in phase for a long time, i.e., many precession periods. If the spectrum is broad, then there are large differences in the precession rates between nuclei. Following an rf pulse, the phase coherence of the nuclei is quickly destroyed by these differences in precession frequencies.

The characteristic time that the nuclei precess in phase, or the characteristic time for the system of nuclei to come to internal equilibrium, is called the spin-spin relaxation time, T2. Since

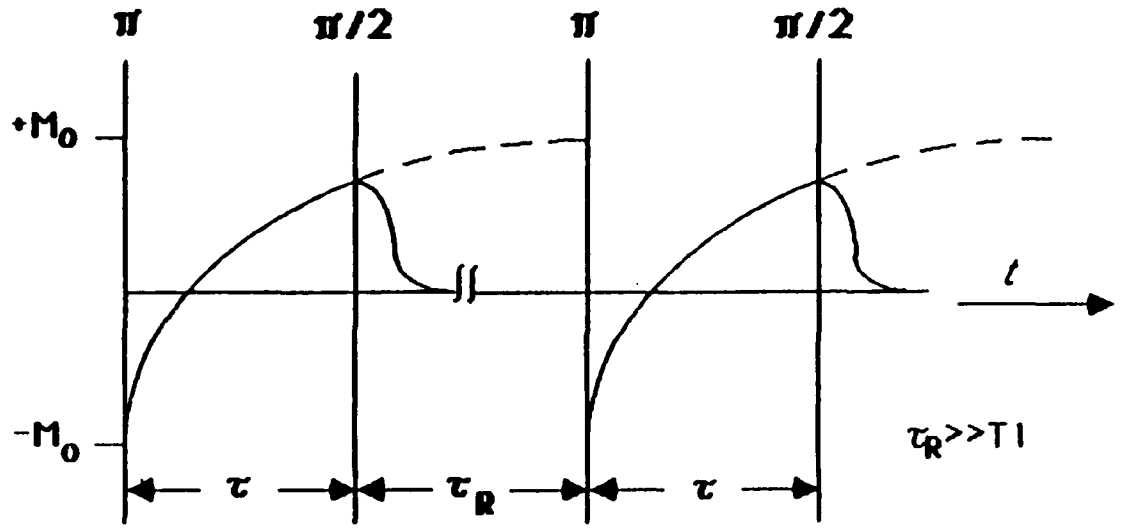

Pulse Sequence for

T1 Measurement

Figure II-3

the nuclei must be at internal equilibrium before they can be at complete equilibrium, then it is obvious that T1, for a given material, is always greater than or equal to T2. For protons in common substances in typical magnetic fields, T2 ranges from tens of microseconds to hundreds of seconds.

In many materials, and especially in solids, experimental estimates of T2 are relatively easy to make. First, the maximum magnitude of the FID is noted. The FID is obscured near the end of the rf pulse due to the finite recovery time of the receiver, so the FID magnitude is recorded just after the receiver system recovers. Then the FID response is followed until its magnitude falls to (1/e) of its former value. The time for this decay is approximately equal to T2, though, in fact, the true value of T2 depends upon the exact shape of the FID.

When NMR samples contain two or more substances, it is common to observe more than one T2 time. A typical example is a solid compound that has absorbed water; one T2 time is observed for the material itself, and one for the absorbed water.

The relaxation times T1 and T2 are important because many explosive compounds possess almost-unique values of these parameters. Therefore, an NMR system may be designed to identify these compounds in the presence of other, benign materials.

G. Solid Echo

Most solid substances exhibit very short T2 times and, as a consequence, much of the FID signal is obscured by the dead time of the NMR system (which is sometimes called the recovery time). A two pulse technique, producing a response called a solid echo, can be used in many cases to recover some of this lost signal.

The solid echo sequence is shown in Figure II-4. At time zero, a 90-degree pulse is applied to the nuclear spin system. Following this pulse, the spin system responds with an FID, but much of the FID signal is obscured by the receiver dead time.

Shortly after the receiver recovers, as shown at time tau in Figure II-4, a second 90-degree pulse is applied. The rf phase of this pulse is shifted by 90 degrees from that of the first pulse. The effect of the second pulse is to produce an NMR response, called a solid echo, which builds in time, goes through a maximum, and then decays to zero. A portion of the solid echo is also obscured by the dead time of the receiver; but if the pulse spacings are properly chosen, then the maximum in the solid echo will be observed, as shown at time 2(tau) in Figure II-4.

The solid echo can be used to improve the signal-to-noise ratio of the system by improving the signal response, and it can also be used to determine the complete shape of the NMR free induction decay. It is anticipated that the solid echo technique will be used in any single-sided NMR system for remote detection.

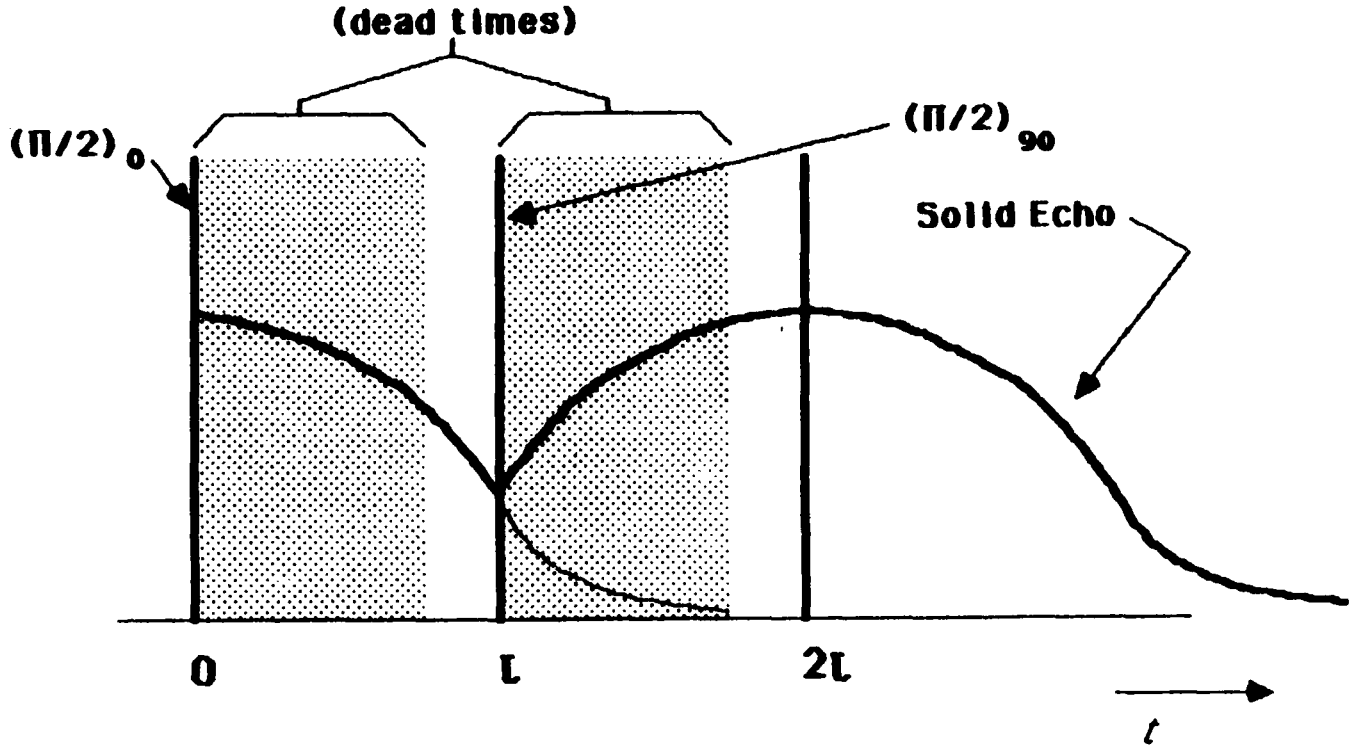

Pulse Sequence for Formation of a Solid Echo

Figure II-4

H. Signal-to-Noise Ratio

The fundamental limit of sensitivity for an NMR system is determined by the signal-to-noise ratio (SNR) of that system. In evaluating the technology, it is important to be able to predict the changes in SNR that will result from changes in other parameters.

Laboratory Systems

For proton NMR systems in typical laboratory configurations, over a wide range of operating parameters, the signal-to-noise ratio scales according to the following expression (12),

$$SNR \propto f(Wo^3QV/B)^{1/2} \qquad (II - 1)$$

where f is the filling factor of the sample circuit (i.e., the ratio of sample to sample coil volumes), Wo is the Larmor frequency, Q is the quality factor of the sample circuit, V is the volume of the sample coil, and B is the bandwidth of the receiver/detector circuitry.

Equation II-1 predicts that the SNR increases as the Larmor frequency to the (3/2) power. In fact, this is a conservative prediction. A comprehensive analysis of the problem (13) resulted in the conclusion that the signal-to-noise ratio varies as the Larmor frequency to the (7/4) power. However, over the range of frequencies under consideration here, the difference between a (3/2) and a (7/4) power dependence is not significant.

Remote Detection Systems

In remote detection NMR, the precessing nuclear magnetization induces a signal voltage, i.e., the FID, into a detector coil. The voltage induced in the detector coil, Es, is given by (6)

$$Es = NQAWoMo/Z^3 \qquad (II - 2)$$

In this expression, N is the number of turns in the detector coil with quality factor Q and cross-sectional area A. In addition, Mo is the total nuclear magnetization precessing at the Larmor frequency Wo, and Z is the center-to-center distance between the remote region of precessing magnetization and the detector coil. It is assumed that the detector coil is aligned in order to maximize the induced voltage Es.

The noise voltage for a remote detection system can be estimated from the well-known expression for Johnson noise. The noise voltage present in the sample circuit is given by

$$En = (4kTBR)^{1/2} \qquad (II - 3)$$

where R is the resistive component of the impedance of the sample circuit, T is the temperature of the sample circuit, B is the bandwidth of the system, and k is Boltzmann's constant.

Combining Equations II-2 and II-3 provides an expression useful for estimating the SNR of prospective remote NMR systems. The voltage signal-to-noise ratio may be written

$$SNR = (Es/En) * F \qquad (II - 4)$$

where F is a term that incorporates all of the factors which may affect the SNR that are not included in Equations II-2 and II-3. Examples of these factors include the effects of the system recovery time and the FID decay time T2, the effect of the length of the rf pulse, the effect of the homogeneity of the rf field over the remote region, the effects of the precise geometry and orientation of the sample coil, and the effects of noise introduced by subsequent amplification of the NMR signal. In general, F is difficult to determine quantitatively. However, under a fairly wide range of conditions, qualitative estimates of F are relatively easy to make.

Recalling that Mo = Mv * Vm, where Vm is the volume of the remote region and Mv is the nuclear magnetization per unit volume, gives

$$SNR = (10^{-5})(5/2k)^{1/2} * (WoMvVm/Z^3) * (NAQ)(TBR)^{-1/2} * F \qquad (II - 5)$$

The first term in Equation II-5 is a constant; the 10^{-5} factor is included to allow use of the convenient units discussed below. The second term is determined by the particular physical configuration of the remote NMR system. That is, a given remote NMR system will result in a given set of the parameters Wo, Vm, and R; and Mv will be determined by the characteristics of the material in the remote region.

The third term in Equation II-5 is determined primarily by the detector coil and its associated circuitry. If the sample circuit is parallel tuned, rather than series tuned, the resistive component of the circuit impedance is given by R = QX, where X is the inductive reactance of the detector coil. With this substitution, the third term becomes

$$\text{Term 3} = (NAQ)(TBR)^{-1/2} = (NA)(Q/TBX)^{1/2}$$

Utilizing X = WoL, where Wo is the Larmor frequency and L is the inductance of the sample coil, and the fact that the maximum Q of the sample circuit, Qm, is limited by the system bandwidth to the value $Qm = Wo/2\pi B$, gives

$$\text{Term 3} = (NA/B)(1/2\pi TL)^{1/2}$$

Over a fairly wide range of parameters, the inductance of the detector coil is expressed by (14)

$$L = CN^2d$$

where L is given in Henries, N is the number of turns, and d is the diameter of the coil in centimeters. The constant C is given by

$$C = (10^{-6}/2.54)/(18 + 40(\ell/d)) \qquad \text{(II - 6)}$$

where ℓ is the length of the coil in centimeters. This expression for C is valid for (ℓ/d) ratios greater than 0.4, and it is unlikely in remote detection NMR that an (ℓ/d) ratio greater than about 2.0 would be encountered. Therefore, the constant C ranges from

$$4.017 \times 10^{-9} < C < 1.158 \times 10^{-8}$$

Incorporating the fact that the area of the coil $A = \pi d^2/4$, gives

$$\text{Term 3} = (1/4B)(\pi d^3/2TC)^{1/2}$$

Substituting this expression into Equation II-5, and collecting the numerical constants into the first term, gives the following equation for the signal-to-noise ratio,

$$SNR = (10^{-5}/8)(5\pi/k)^{1/2} * (WoMvVm/Z^3) * (1/B)(d^3/TC)^{1/2} * F \qquad (II - 7)$$

The numerical values and units for the terms used in Equation II-7 are given below.

k = Boltzmann's Constant,
= 1.38×10^{-23} ergs/Kelvin;

Wo = Larmor frequency, in radians/second,
= 2.675×10^7 at Ho = 1,000 Gauss;

Mv = Nuclear magnetization per unit volume in the sensitive region, in abamp/cm,
= 3.170×10^{-7} (for 6.6×10^{22} spins/cc, Ho = 1,000 Gauss, and Sample Temp = 300 K);

Vm = Volume of sensitive region, in cm^3;

Z = Center-to-center distance between pickup coil and sensitive region, in cm;

d = Diameter of pickup coil, in cm;

B = Bandwidth of the detection system, in Hertz;

T = The temperature of the sample circuit source resistance, in degrees Kelvin;

C = A unitless constant that depends upon the geometry of the pickup coil, given by Equation II-6;

F = A unitless term incorporating all of the factors that affect the SNR not otherwise included in Equation II-7.

III. NMR AND THE MATERIALS OF INTEREST

A. Introduction

Differences in the NMR relaxation properties of materials form the basis for NMR methods of explosives detection. Therefore, a general appreciation of the reasons why different materials exhibit different NMR properties is central to an understanding of the detection technique. In the following discussion, all comments and quantities apply specifically to proton NMR, and not to NMR characteristics of other nuclei.

In general, the relaxation time T1 for protons is influenced by: (a) the strength of the magnetic interaction between a given proton and its neighbors; and, (b) the relative motion between the proton and its neighbors. When the frequency of this relative motion is at, or very near, the Larmor frequency, then T1 is short. When the frequency of this motion is either much higher or much lower than the Larmor frequency, then T1 is long. The strength of the magnetic interaction depends primarily upon the nearest neighbor distances between nuclei and upon the presence, or absence, of paramagnetic impurities.

If the molecular motion near the Larmor frequency is simple, i.e., if there is only a single type of motion and all nuclei participate, then the behavior of T1 is relatively easy to characterize. The behavior of T1 is generally discussed in terms of t, the correlation time for the molecular motion. If, for example, the molecular motion is translational diffusion, then the correlation time, t, can be thought of as the time between diffusional jumps. Or, if the motion is molecular reorientation, then the correlation time can be thought of as the average time it takes for a molecule to rotate through an angle of one radian. In a broad sense, the correlation time may be thought of as the inverse of the frequency of the molecular motion.

Figure III-1 is a log-log plot of T1 versus the correlation time t for three different Larmor frequencies (A, B and C). In the region of short correlation times, i.e., for high temperatures in most substances, the frequency of molecular motion is much higher than the Larmor frequency. Here, the T1 of the material is long and increases as the correlation time decreases. Also, in this region, T1 is independent of the Larmor frequency chosen.

When the frequency of molecular motion is roughly equal to the Larmor frequency, T1 goes through a minimum. Since Larmor frequencies can be altered experimentally by changing Ho, separate T1 minima may be observed and these are shown in Figure III-1.

When the correlation times are long, i.e., at low temperatures, where the frequency of molecular motion is low compared to the Larmor frequency, then T1 is again long and lengthens with

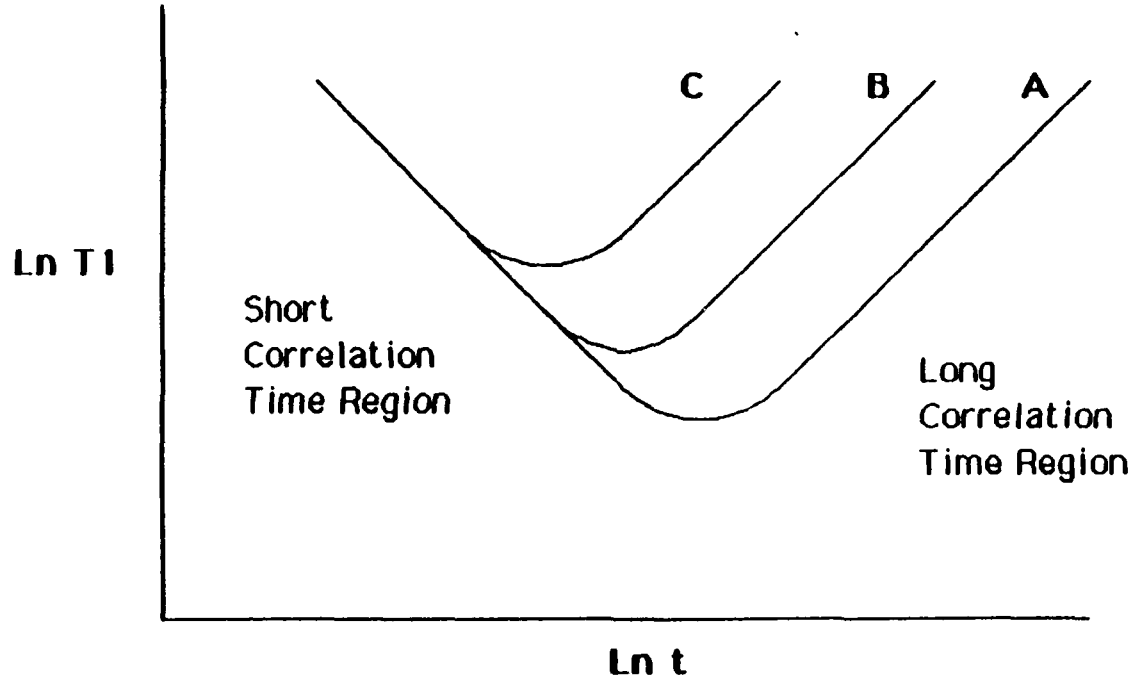

Spin-lattice Relaxation Time versus Correlation Time for Molecular Motion

Figure III-1

increasing correlation time. However, in contrast to the short correlation time region, the specific value of T1 in this region depends upon the specific Larmor frequency chosen for observation. Therefore, some indication of the nature of the molecular motion can be obtained through studies of the Larmor frequency dependence of T1 relaxation times.

The relaxation time T2 is a rather complex function of the two parameters that influence T1, i.e., the frequency of molecular motion and the strength of the internuclear coupling. However, in general, T2 is long if the coupling between nuclei is weak, and short if the coupling is strong. Both T1 and T2 times are influenced by changes in the temperature of the substance, since temperature changes affect the frequency of molecular motion. T1 and T2 are also sensitive to the choice of Larmor frequency, since a Larmor frequency near a frequency of molecular motion results in a short T1.

Of all the possible molecular motions occurring in common substances, three often occur at rates close enough to the Larmor frequency to influence T1 and T2. These three motions are: (a) molecular tumbling, (b) molecular diffusion, and (c) reorientation of mobile groups internal to the molecule. One, or more, of these three motions generally determines the observed values of the relaxation times.

In liquids, molecular diffusion, tumbling, and possible internal motions usually proceed at rates fast compared to the Larmor frequency and, therefore, T1 is usually long (i.e., longer than, say, 500 milliseconds). In addition, since the molecules are in rapid motion relative to one another, the coupling between nuclei is weak and T2 is also long. In fact, in many simple liquids, T1 and T2 are often equal.

In solids, molecular diffusion and tumbling usually proceed at rates slow compared to the Larmor frequency. Therefore, in rigid crystalline solids, T1 is generally long. In addition, since the atoms are fixed in place and the nuclei are essentially stationary, the coupling between nuclei is strong and T2 is short (15).

However, most solids are not rigid crystalline materials. Most common substances are, in fact, composed of complex molecules that possess side chains capable of a wide variety of internal motions. If many side chains are present, then it is likely that some internal motions will take place near, or above, the Larmor frequency (16). And, of course, the longer the side chains, the more likely it is that some internal motions will occur near the Larmor frequency. Therefore, T1 in most common solid substances is short (i.e., less than about 500 milliseconds) and, since T2 is always less than or equal to T1, T2 is also short.

B. Mixtures of Compounds

In use, an NMR detection system will often encounter many different materials simultaneously. Therefore, it is important to determine the response of the system in the presence of two or more compounds.

The NMR relaxation time, or times, exhibited by a mixture of compounds may be difficult to analyze, or to predict, quantitatively. The results depend, in large part, upon whether or not the molecules of the compounds are in intimate contact. If not, and even if the compounds are in very close proximity, then the situation is described by the separate responses from each of the components of the mixture. If so, then the situation is described by a somewhat more complex combined response. Each of these two situations is discussed below.

Separate Compounds

The description of the relaxation process when a number of separate, noninteracting compounds are involved is fairly straightforward. The case of two separate compounds is outlined here, and these results are readily generalized to account for additional compounds.

Assume that the two compounds, A and B, are allowed to come to equilibrium in the static magnetic field and a 180 degree pulse is applied. The nuclear magnetization, which was Mo before the pulse, is rotated to -Mo immediately afterward (see Chapter II, Section E). At time t later, a 90 degree pulse is applied and the Z-component of the magnetization, Mz(t), is determined from the FID height.

The return to equilibrium of the Z-component of the magnetization is given by the following expression:

$$(Mo - Mz(t))/2Mo = Ae^{-t/Tl(A)} + Be^{-t/Tl(B)}, \qquad (III - 1)$$

where A is the mole fraction of compound of compound A, B is the mole fraction of compound B, Tl(A) is the spin-lattice relaxation time of compound A, and Tl(B) is the spin-lattice relaxation time of compound B.

Although it is difficult to solve Equation III-1 in general, the solution is easy to determine in specific regions. For example, when A is much greater than B, then the observed Tl of the separate compounds, Tl(SC), is approximately equal to Tl(A). Similarly, when B is much greater than A, then Tl(SC) is approximately equal to Tl(B).

It is important to note, however, that an NMR explosive detection instrument based upon T1 differences will not respond to the (1/e) time, or T1 time, calculated from Equation III-1 for a given mixture. Rather, the instrument will respond to the separate FID magnitudes and T1 times of the individual components of the mixture falling within the instrument response window.

Mixed Compounds

If the molecules of the two compounds are in intimate contact, as in solid solutions, then the state of the relaxation process in one compound is transmitted to the other, and vice versa. This communication takes place in a time on the order of T2. In the limit where T2 is short, i.e., the communication is fast, then the resulting relaxation rate is given by:

$$1/T1(MC) = A/T1(A) + B/T1(B), \qquad (III - 2)$$

where T1(MC) is the relaxation time for the mixture and the other symbols have the same meanings as in Equation III-1.

In order for Equation III-2 to apply, the two compounds must be mixed on a molecular level. Therefore, it is extremely unlikely that T1(MC), from Equation III-2, would accurately describe the relaxation observed in the simple mixture of, for example, two powders.

It is not out of the question, however, that situations could arise which would require a combination of Equations III-1 and III-2 for an accurate description. Quantitative analysis of these situations would be difficult.

C. Explosive Compounds

Many explosive compounds are structurally rigid and as a result, exhibit long proton relaxation times. In addition, many explosives contain nitrogen, and the nitrogen atoms are often situated in close proximity to hydrogen atoms. As a consequence, explosive compounds often exhibit a relaxation effect called hydrogen nitrogen level crossing which arises from an interaction between the two types of nuclei.

Nitrogen nuclei possess a quadrupole moment and tend to align along electric field gradients in the material. This alignment produces nuclear quadrupole resonance (NQR) frequencies which, under certain conditions, may be equal to the proton resonance frequency. By adjusting the Larmor frequency, or magnetic field, the hydrogen and nitrogen nuclei can be brought into in thermal contact and can exchange energy. This is called level crossing.

The T1 of the nitrogen nuclei is generally much shorter than the T1 of the hydrogen nuclei. The energy exchange at the level crossing frequency shortens the proton T1. The result is that many explosive compounds exhibit short proton T1 times at certain specific Larmor frequencies and long T1 times elsewhere.

The chemical properties and structures of a variety of explosive compounds are discussed below. If NMR relaxation times for these compounds were available, they are included along with comments on important considerations related to the NMR detection process.

Black Powder

Black powder is a simple mixture of potassium nitrate, charcoal and sulfer. It contains little or no hydrogen. Therefore, black powder is not detectable by proton NMR.

Compound B

Compound B is a cast explosive (18). That is, it is cast from a mixture into predetermined shapes. Compound B is an intimate mixture of approximately 40% TNT and 60% RDX. Some formulations may include up to 63% RDX and 1% of an unspecified wax.

It should be possible to estimate the NMR properties of Compound B from the NMR properties of its major constituents. The known NMR properties of TNT and RDX are given below, and the guidelines for estimating the relaxation properties of mixtures are discussed in Section B of this chapter.

Compound C-4

Compound C-4, sometimes called Harrisite and more often by the generic name "plastic explosive", is a simple mixture of 91% RDX,

5.3% Di(2-etnylhexyl) sebacate, 2.1% polyisobutylene, and 1.6% motor oil (18). The NMR properties of Di(2-ethylhexyl) sebacate are unknown. The NMR properties of polyisobutylene have been recently measured (17) and this rubbery polymer exhibits a relatively short T1 of about 30 milliseconds near room temperature. The T1 of motor oil is unknown but is likely to be a few seconds or less.

Since Compound C-4 is a simple mixture of these four compounds, its NMR relaxation properties likely approximate those of RDX, its major constituent.

HMX

HMX, or 1,3,5,7-tetranitro-1,3,5,7-tetrazacyclooctane, is a pure explosive compound and the major constituent in a number of plastic-bonded explosives (18). The chemical structure of HMX is shown in Figure III-2.

The NMR properties of HMX are not available. However, the chemical structure suggests that, in the solid form, molecular motions are likely to be slow. Therefore, T1 is expected to be long. In addition, the presence of a large number of nitrogen atoms indicates that significant hydrogen/nitrogen level crossing effects may occur.

PETN

Pentaerythritol tetranitrate, or PETN, is a white, moldable compound with eight hydrogen and four nitrogen atoms per molecule and a molecular weight of 316 (18). The chemical structure of PETN is shown in Figure III-3.

PETN is a sensitive and very powerful explosive with a detonation velocity of 8,100 meters/second (19). It is used extensively in detonating cords and, at times, as a primary or an intermediary charge.

PETN exhibits a long T1 at Larmor frequencies considered suitable for NMR detection (2). At 3 MHz, the proton T1 is approximately 60 seconds. In common with many explosives, PETN also exhibits hydrogen/nitrogen level crossing. Level crossing occurs at proton Larmor frequencies of 0.50 and 0.90 MHz which correspond to applied magnetic fields of 117 and 211 Gauss, respectively.

RDX

RDX, or 1,3,5-trinitro-1,3,5-triazocyclohexane, is a white moldable compound with six hydrogen and six nitrogen atoms per molecule and a molecular weight of 222 (18). RDX is the major component of the often-used plastic explosive C-4. The chemical structure of RDX is shown in Figure III-4.

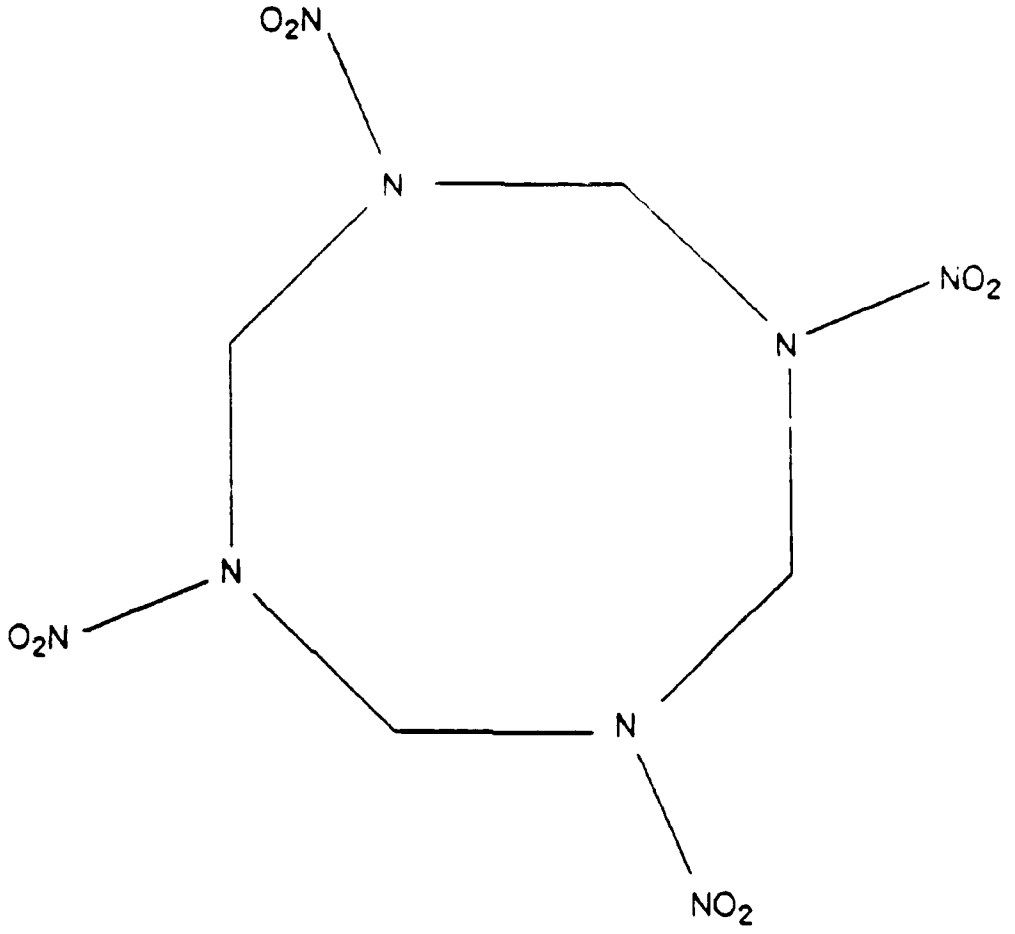

1,3,5,7-Tetranitro-1,3,5,7-tetrazacyclooctane (HMX)

Figure III-2

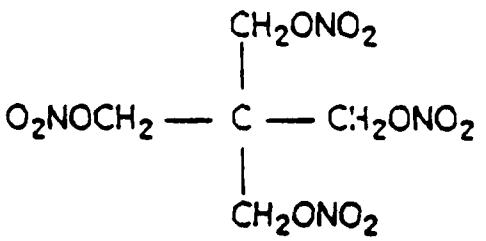

Pentaerythritol tetranitrate
(PETN)

Figure III-3

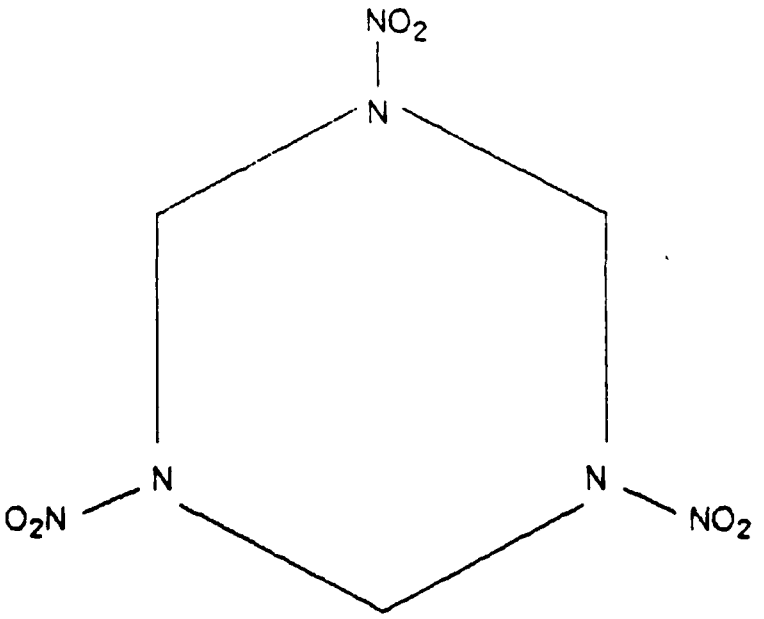

1,3,5-Trinitro-1,3,5-triazocyclohexane (RDX)

Figure III-4

RDX, originally developed as a medicine (20), exhibits about the same explosive power as PETN. However, RDX is considerably more stable chemically and is much less sensitive to mechanical shock (19).

RDX exhibits very long T1 times at Larmor frequencies considered suitable for NMR detection. At 3 MHz, the proton T1 of RDX is 312 seconds at 3 MHz (2).

RDX also exhibits a hydrogen/nitrogen level crossing effect which lowers the proton T1 time at certain values of the applied field. Level crossing occurs (2) at fields of 423, 798 and 1,221 Gauss, which correspond to proton Larmor frequencies of 1.8, 3.4 and 5.2 MHz, respectively.

TATB

TATB, or 1,3,5-triamino-2,4,6-trinitrobenzene, is a bright yellow pure explosive compound with the chemical structure indicated in Figure III-5 (18).

The proton NMR relaxation properties of TATB were determined by Garroway and Resing (21). At a Larmor frequency of 60 MHz, TATB exhibits fairly constant proton T1 times of about 30 seconds over a wide range of temperatures indicating little molecular motion at high frequencies. No data were available concerning hydrogen/nitrogen level-crossing effects in TATB.

TNT

TNT, or 2,4,6-trinitrotoluene, is a light brown compound with five hydrogen and three nitrogen atoms per molecule and a molecular weight of 227 (18). TNT is considerably less powerful, and less sensitive, than RDX (19). The chemical structure of TNT is shown in Figure III-6.

Compared to PETN and RDX, TNT exhibits shorter T1 times at the Larmor frequencies appropriate to NMR detection (2). At 3 MHz, the proton T1 of TNT at 3 MHz is approximately 25 seconds.

Level-crossing fields in TNT are comparable to those found in PETN. Hydrogen/nitrogen level crossing occurs at applied fields of 185 and 204 Gauss. These fields correspond to proton Larmor frequencies of 0.79 and 0.87 MHz, respectively.

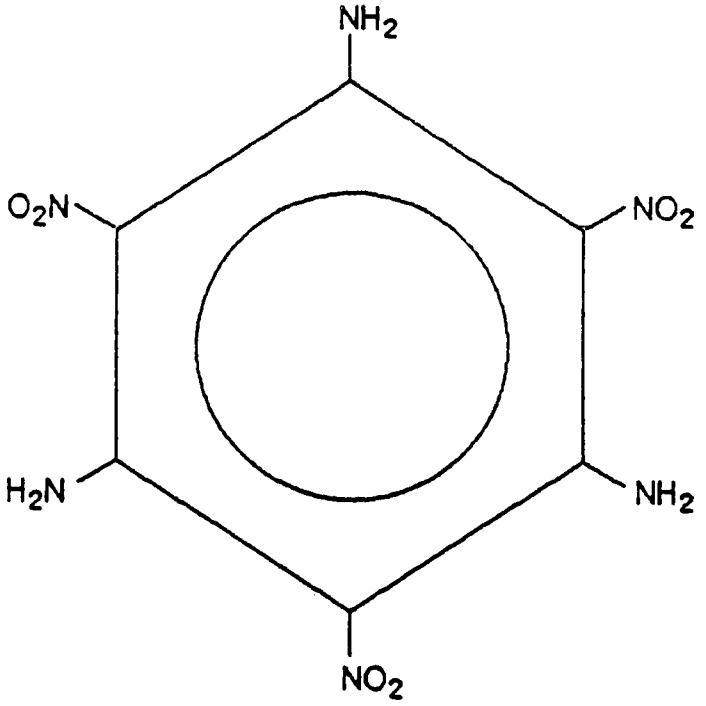

1,3,5-Triamino-2,4,6-trinitrobenzene
(TATB)

Figure III-5

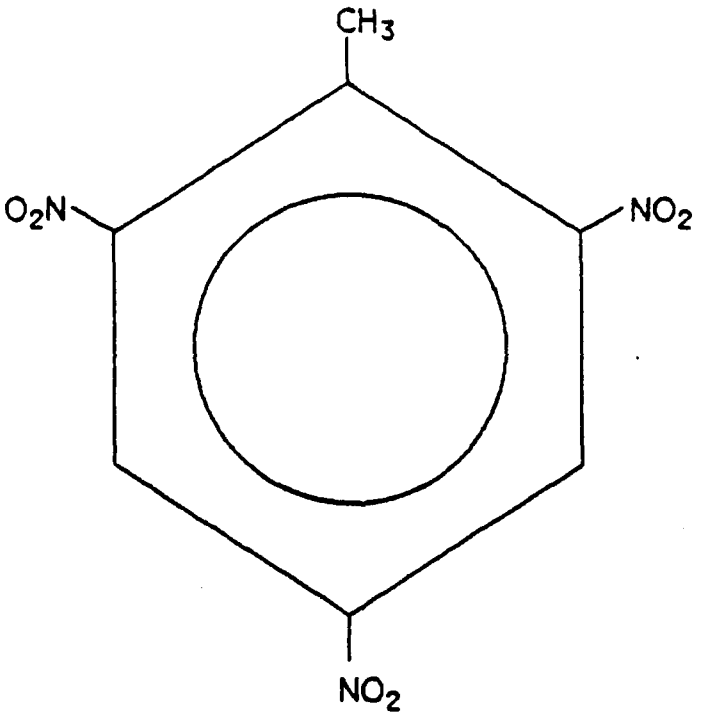

2,4,6-Trinitrotoluene (TNT)

Figure III-6

D. Benign Substances

The molecular structures and NMR properties of some of the benign substances that may be encountered during the inspection process are discussed below. It should be noted that few, if any, of these materials will exhibit the hydrogen/nitrogen level crossing effects characteristic of many explosives.

Bakelite

Bakelite is a thermosetting phenol formaldehyde resin often used as an electrical insulator. The chemical structure of bakelite, which appears to be quite rigid, is shown in Figure III-7.

Though no NMR data are available, the bakelite structure suggests that molecular motions are restricted. Therefore, it is likely that T1 times in bakelite are long.

Glass

Glass is a silicate and contains no protons. Therefore, there is no proton NMR response from glass.

Metals

The presence of metals will interfere with the NMR inspection process. At best, the sensitivity of the NMR instrument may be reduced. At worst, no signal at all will be received.

For example, if an explosive is placed in a metal container or wrapped in metal foil, there will be no response from the NMR instrument. On the other hand, the presence of metal items, or of metal foil that does not enclose the explosive, will produce a loss of sensitivity that may or may not be nominal, depending upon the relative placement and orientation of the materials.

Plexiglas

Polymethyl methylacrylate is a hard clear thermoplastic polymer with trade names such as Plexiglas and Lucite. The structure of polymethyl methylacrylate is shown in Figure III-8. At room temperature and at a Larmor frequency of 19 MHz, Plexiglas exhibits a T1 of 88 milliseconds (22).

Polymethyl methylacrylate has short simple side chains that terminate in methyl groups. This is a molecular structure capable of exhibiting a wide range of internal motion frequencies in the solid state, and these motions are, no doubt, responsible for the short T1 times observed for this compound.

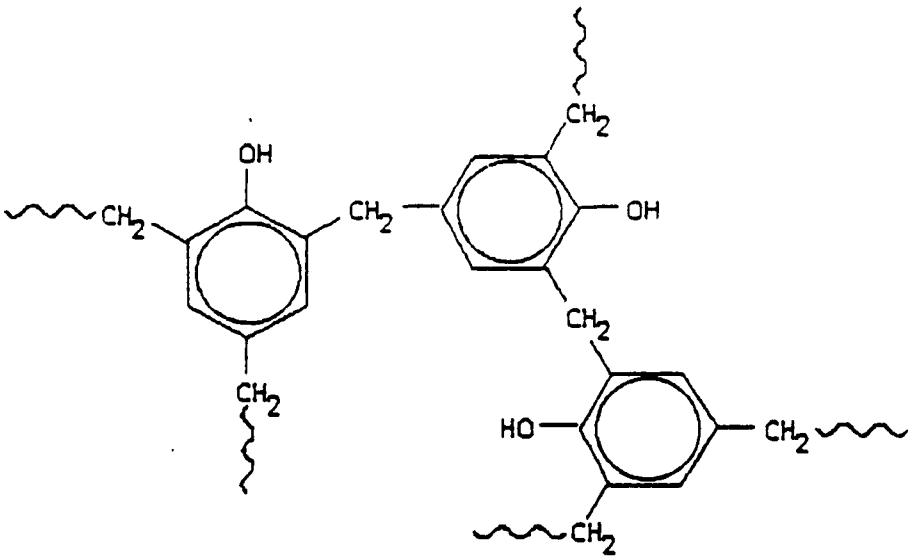

Bakelite
(phenol-formaldehyde resin)

Figure III-7

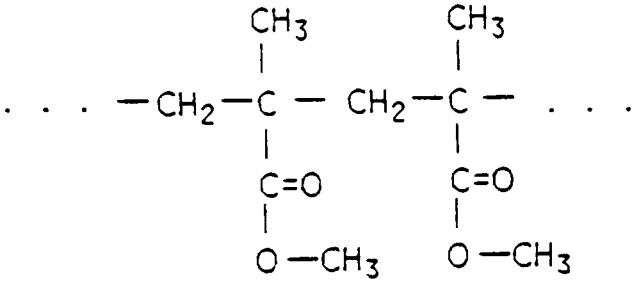

Molecular Structure of
Polymethyl methylacrylate

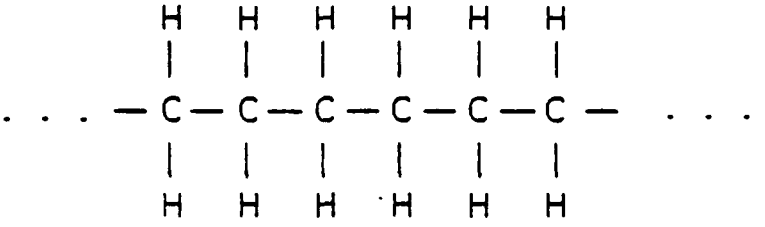

Molecular Structure of Polyethylene

Figure III-8

Polyethylene

Polyethylene is a soft clear thermoplastic polymer with the structure shown in Figure III-8. It is a very simple linear polymer with a repeating group consisting of one carbon and two hydrogen atoms. A single T1 measurement at room temperature and 19 MHz gave 92 milliseconds (22).

The opportunities for complex motions are limited in polyethylene, but "crankshaft" rotations and chain end diffusion may occur over a wide range of frequencies. The presence of these motions is likely the reason for the short T1 observed in this compound.

Rubber

The structure of polyisoprene, or natural rubber, is shown in Figure III-9. T1 times observed in rubber are quite short, e.g., 34 milliseconds at 19 MHz at room temperature (22).

This compound possesses a simple repeating unit with very simple side chains. Both the side chains and the repeating units are capable of a wide range of motional frequencies, and this is consistent with the experimental observation of very short T1 times.

Styrofoam

The principal, and perhaps only, component of styrofoam is polystyrene. The structure of polystyrene is shown in Figure III-10. T1 times for styrofoam at 19 MHz (22) range from 0.75 to 0.82 seconds which are somewhat longer than those observed for many other polymer compounds.

Polystyrene is a linear polymer with a carbon backbone. Phenyl groups are connected to every other carbon on the chain. The size of the phenyl groups hinders many of the possible modes of molecular motion and likely slows down side chain reorientations and "crankshaft" rotations considerably.

Vinyl Materials

Vinyl polymers are used to fabricate a wide variety of items. A typical example is electrical tape, which is an adhesive-backed vinyl compound. The measured T1 time for electrical tape is 122 milliseconds at room temperature and a Larmor frequency of 19 MHz (22). Compared to the T1 times for explosives, the relaxation times for vinyl compounds are likely to be very short.

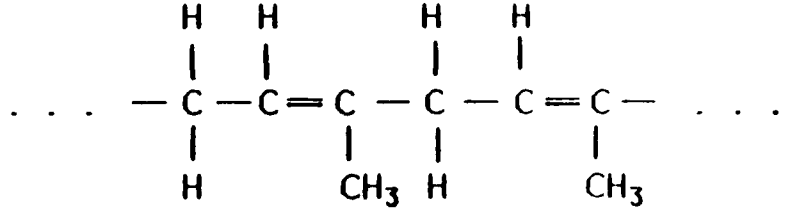

Molecular Structure
of Polyisoprene

Figure III-9

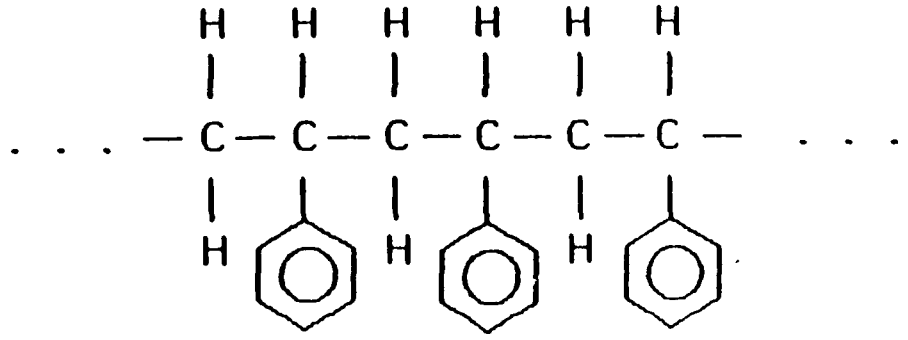

Molecular Structure of Polystyrene

Figure III-10

Wood Paper

The principal constituent of wood and paper is cellulose. A Haworth diagram of the repeating unit of a cellulose chain is shown in Figure III-11. In both wood and paper, these chains are of irregular length and are arranged in an amorphous fashion.

Wood and paper exhibit short T1 times over a wide range of Larmor frequencies (22). An examination of Figure III-11 indicates that a variety of molecular motions are possible in cellulose, including side chain reorientation, "crankshaft" rotations of a group of repeating subunits, and end-of-chain diffusive motions. These likely occur over a wide range of frequencies and give rise to the observed relaxation behavior.

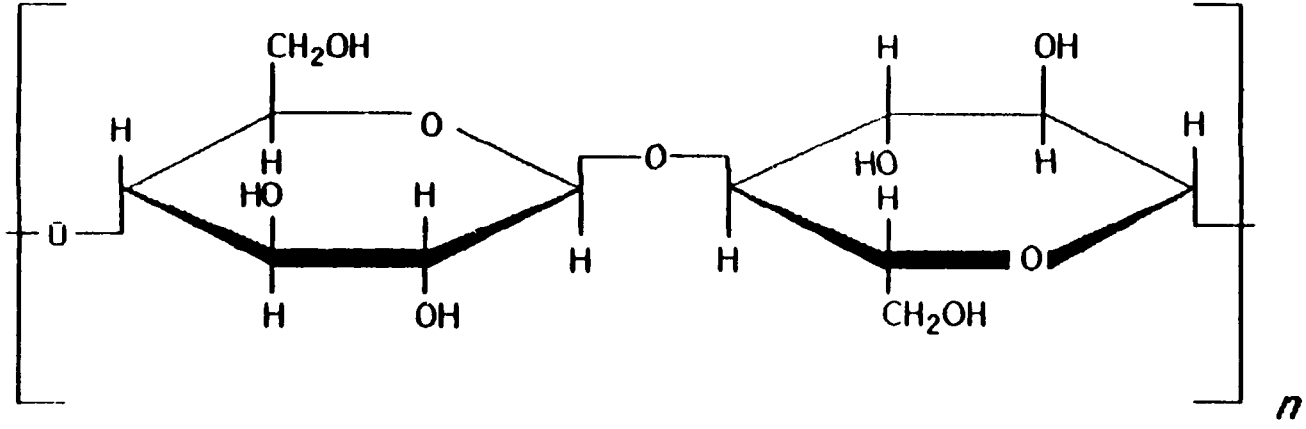

Haworth Diagram of Repeating Subunit of Cellulose Polymer

Figure III-11

IV. SYSTEM COMPONENTS FOR REMOTE NMR

A. Introduction

The purpose of this program is to explore and evaluate the potential of nuclear magnetic resonance (NMR) for remote detection applications. Regions that are accessible from only one side are of particular interest.

Single-sided NMR remote detection systems differ from laboratory NMR systems in that the required region of homogeneous DC field, i.e., Ho, must be produced remotely. The required rf field, H1, must also be produced remotely. As in the case of laboratory NMR systems, H1 in remote detection systems must be directed perpendicular to the steady field Ho.

The following section of this chapter presents alternate methods of producing remote regions of DC magnetic field. The third section of this chapter discusses alternate methods for producing remote regions of rf field. In the final section, a figure-of-merit is defined which allows comparison of alternate systems of NMR remote detection.

B. DC Field Configurations

An NMR system must be capable of producing a magnetic field that is constant in time, i.e., a DC magnetic field. In most cases, it is desirable that this DC field be homogeneous in the region to be examined. In the case of a single-sided NMR system, this homogeneous region of steady magnetic field must be produced remotely.

Several alternate methods of producing remote fields are discussed in the following sections. First, the toroidal geometry of Inside-Out NMR is presented. Then, a discussion of U-shaped iron magnet technology is followed by a detailed treatment of opposed coils and solenoids.

Opposed Magnet Configuration

An opposed magnet configuration, termed Remote Inside-Out NMR, was developed as a tool for borehole logging (5,6,7). The homogeneous region of magnetic field is produced by placing two magnets along a line, as shown in Figure IV-1 (7). The line is a line of symmetry for the system, and the poles of the two magnets are opposed.

This configuration results in a toroidal region of homogeneous field. The toroidal region of homogeneous field is produced in the plane that is equidistant between the two magnets and

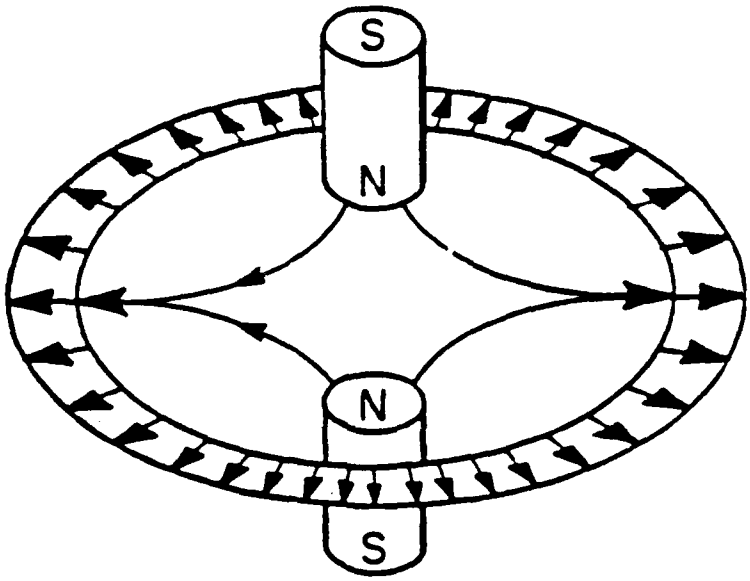

OPPOSED MAGNETS PRODUCE REGION OF HOMOGENEOUS RADIAL MAGNETIC FIELD NEAR MIDPLANE

Figure IV-1

perpendicular to the line connecting them. The field is directed radially outward, perpendicular to the line of symmetry.

In practice, the homogeneous region of field may be produced by permanent magnets, electromagnets, or superconducting coils. However, since the homogeneous region results from magnets in opposition, the maximum field strength is limited. This is illustrated by the data (7) shown in Figure IV-2.

In this example, an electromagnet capable of a maximum field strength of about 15 Kilogauss in a typical laboratory configuration produced a homogeneous field of only about 120 Gauss in the opposed magnet configuration. In the laboratory configuration, the field was produced over a region 10 cm in diameter and 2.5 cm long, i.e., a 2.5 cm pole face gap. In the opposed magnet configuration, the field was produced over a toroid approximately 14.5 cm in diameter, with a cross-sectional diameter of approximately 3 cm.

U-Shaped Magnet Configuration

Magnets with U-shaped yokes can be used to produce magnetic fields in remote regions. Both electromagnets and permanent magnets are suitable. A sketch of such a system is shown in Figure IV-3.

The U-shaped yoke configuration has been recently used in NMR systems to measure moisture levels in structural concrete and in subsurface soils (3,4). The remote region of magnetic field is not as well defined as that produced by the opposed magnet configuration and, in addition, is not as homogeneous. That is, field gradients within, and near, the region of constant field are greater in the U-shaped configuration than in the opposed magnet configuration.

In fact, the cylindrical region of uniform field sketched in Figure IV-3 represents a gross simplification of the actual situation. Between the two poles, within the indicated region of uniform field, the lines of constant field actually conform to the shape of a saddle.

The maximum strength of the remote field produced by a U-shaped magnet configuration would naturally be expected to be somewhat greater than that produced by configurations of opposed magnets or coils. Available information on the system used to measure moisture levels in concrete indicates that this is, in fact, the case.

The inside dimension of the iron yoke for the magnet used in the system for concrete moisture level measurements is 11 inches (27.9 cm). At maximum current, this system produces a field of 494 Gauss at a maximum remote distance of 6 inches (15.2 cm). This distance is very close to the diameter of the remote field toroid in the opposed magnet example discussed above. The field

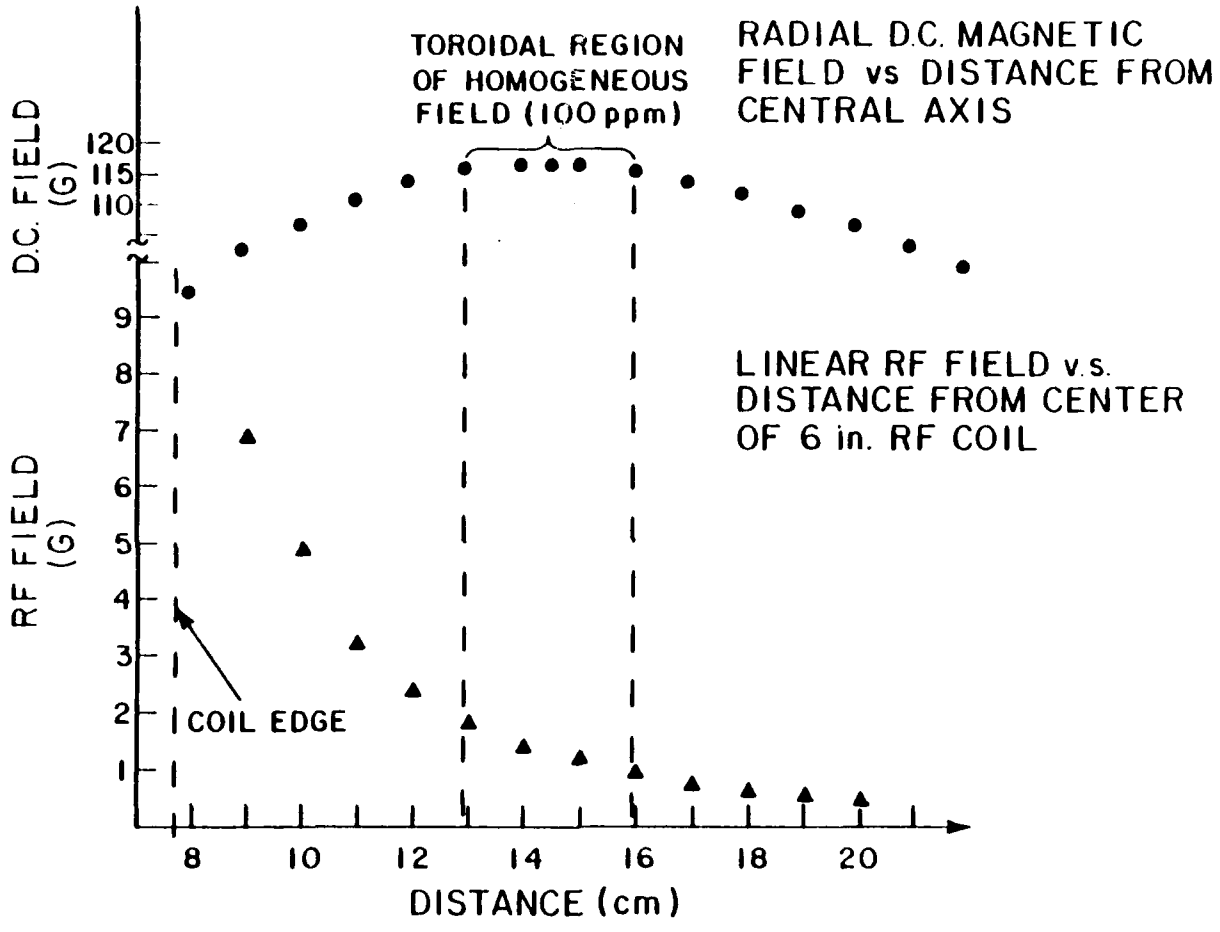

Figure IV-2

DC and RF Field Strengths
Versus Radial Distance

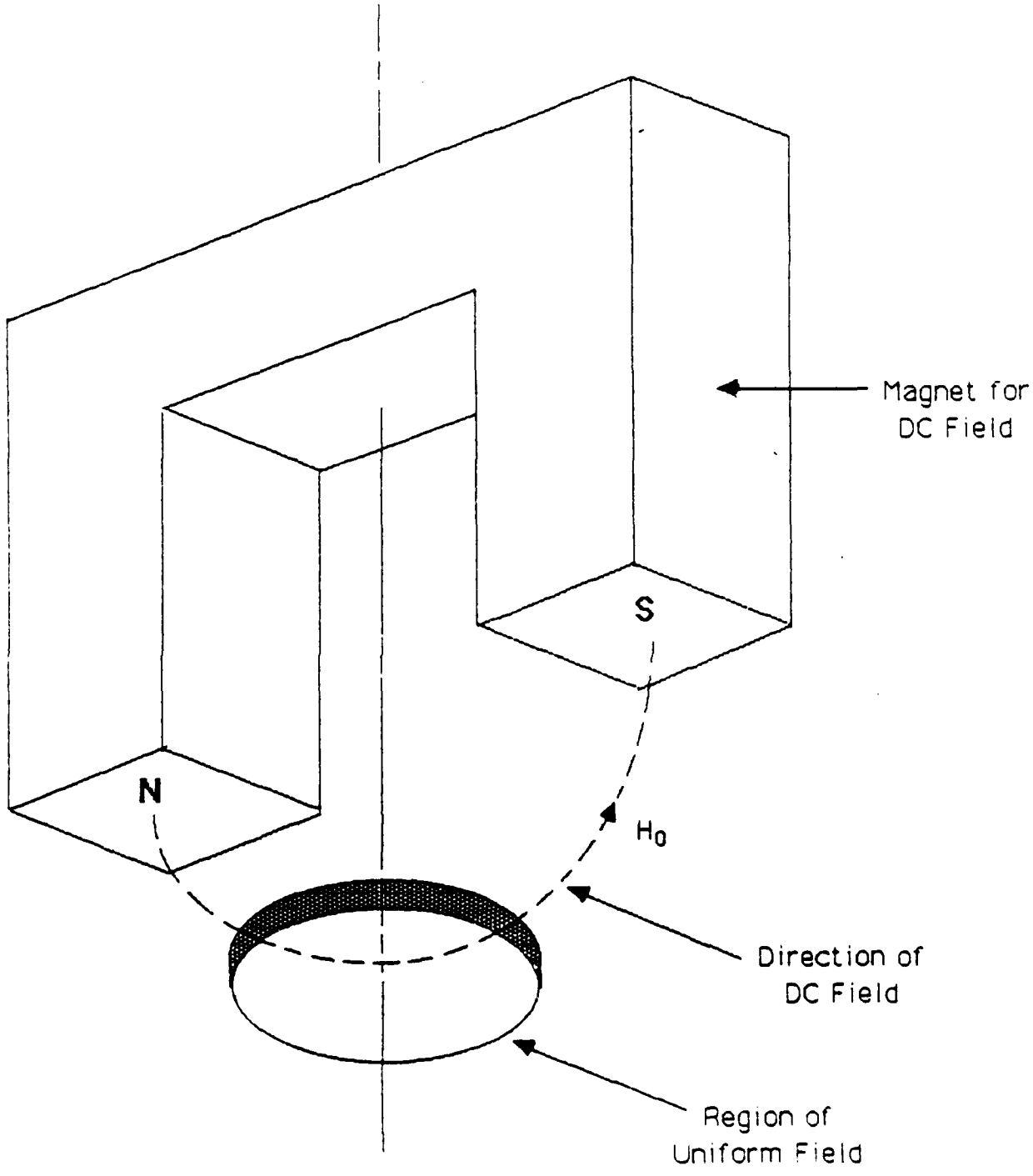

Figure IV-3

An Electromagnet With a U-Shaped Yoke
Produces a Remote Region of Uniform Field

strength in the remote region, though, exceeds that of the opposed magnet example by more than a factor of four.

Opposed Coil and Solenoid Configurations

Current-carrying coils and solenoids can also be used to produce remote regions of homogeneous magnetic field. In particular, configurations of coils and solenoids designed to produce fields that partially cancel may be particularly useful (2,23). These configurations are commonly called opposed coils or opposed solenoids.

A schematic of an opposed coil pair is shown in Figure IV-4. The system consists of two concentric coils of different radii. In the coordinate system used here, the center of the coils is assumed to be the origin, and the Z-axis is perpendicular to the plane of the coil windings. The currents in the coils flow in opposition; that is, they produce magnetic fields which tend to cancel.

Since the radii of the two coils are different, the fields that they produce will not cancel in all regions of space, even if they cancel in a specific region. For example, assume that the currents are adjusted so that the magnetic field at the origin of the coordinate system is zero. Along the Z-axis, the field due to the inner coil will fall off more rapidly with increasing Z than the field due to the outer coil. Therefore, as Z increases from the origin, the total magnetic field, i.e., the vector sum of the fields from each of the two coils, must first increase.

However, when Z becomes large, the fields from each of the coils go to zero and, hence, the total field is zero. Therefore, along the positive Z-axis, the magnetic field from this coil pair is zero at the origin, increases with increasing Z, goes through a maximum, and then falls back to zero.

This behavior is shown in the plot of Figure IV-5. The point of maximum field occurs at a distance Zm from the origin. The precise location of Zm depends upon the ratio of the radii of the two coils and the ratio of the two current flows. In this example, the radius of the larger coil is assumed to be 10 units and that of the smaller coil 5 units. Each produces a field of unity magnitude at the origin. The maximum in the resultant field, with a magnitude of 0.369, occurs at 5.73 units along the Z-axis.

About the point Zm, the homogeneity of the magnetic field can be expressed within specified limits. The size of the region of homogeneous field, i.e., the homogeneous volume, depends not only upon the limits specified, but also upon the ratios of the coil radii and current flows.

The three dimensional shape of the homogeneous region is quite complex. To a crude approximation, though, the homogeneous

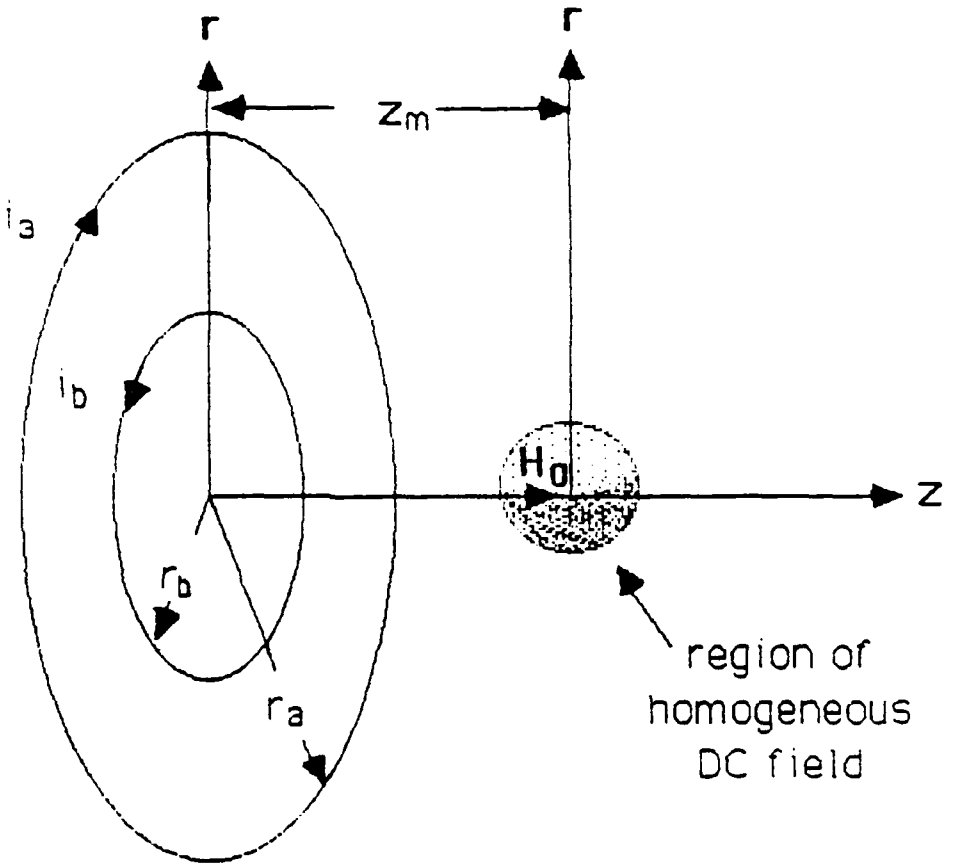

Opposed Coils

Figure IV-4

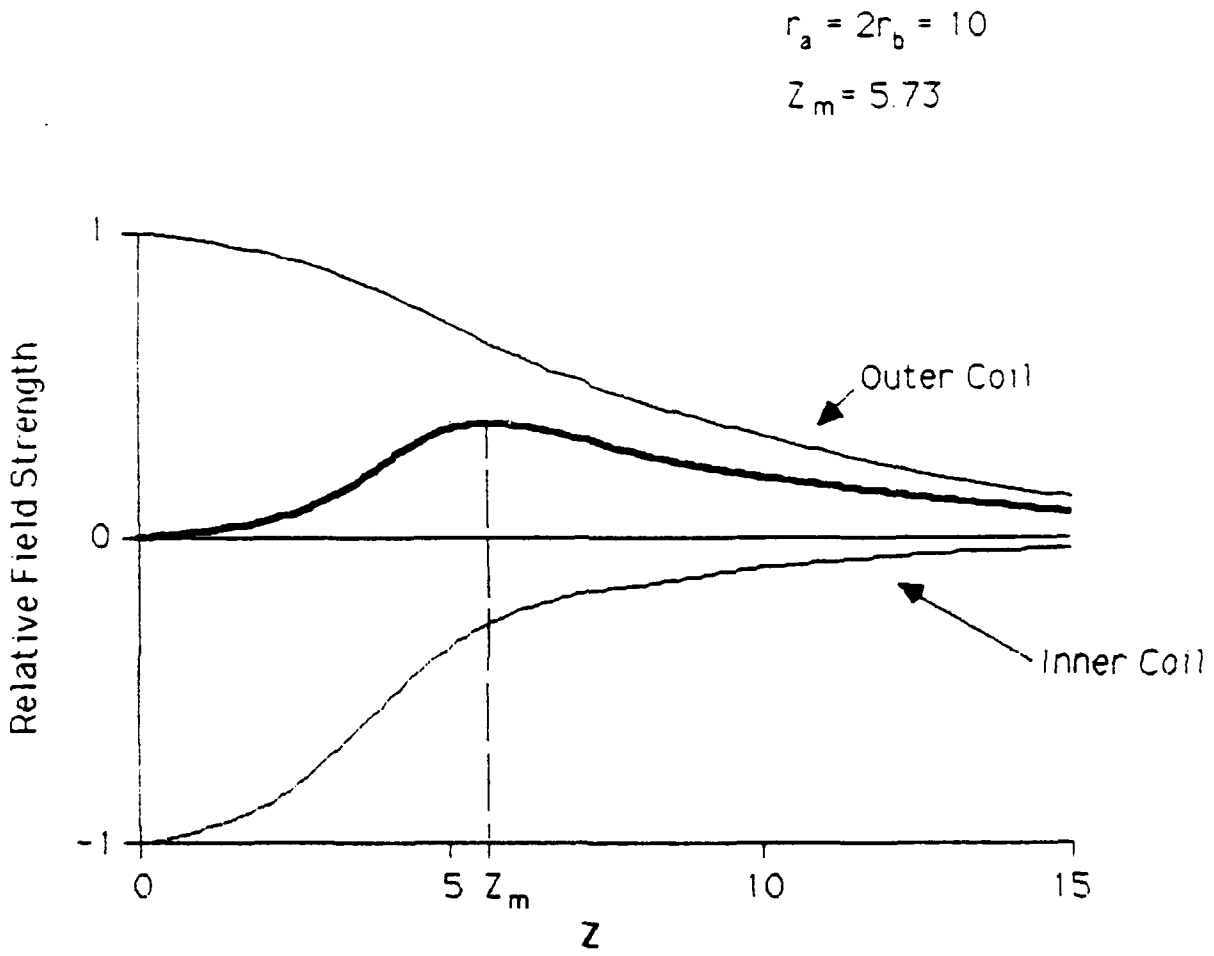

Resultant Field From
Two Opposed Loops

Figure IV-5

region can be assumed to be spherical in shape. This approximation was made in the analyses that follow in a later section.

The magnitude of the field at its maximum and the size of the homogeneous region can be altered by offsetting the two coils from one another. This is shown in Figure IV-6, which is a sketch of opposed coils offset by a distance S. The origin, i.e., Z = zero, is assumed to be at the center of the coil closest to Zm, the point of the remote field maximum. The configuration shown in Figure IV-6 is termed a negative shift. If S extends in the -Z direction, this is termed a positive shift.

It is of interest to note that there are particular combinations of coil radii, coil currents and offset distances that produce a region around the point Zm where not only the first derivative but also the second derivative of the field with respect to distance goes to zero. By analogy to Helmholtz coils, these are called Inside-Out Helmholtz configurations (23).

Inside-Out Helmholtz coils produce a larger region of homogeneous field than do pairs of coils with arbitrary spacing and currents. A sketch of an Inside-Out Helmholtz pair is shown in Figure IV-7, and the corresponding plot of fields along the Z-axis is shown in Figure IV-8. Inside-Out Helmholtz opposed coils require a positive shift, which means that the smallest of the two coils is closest to the remote region of homogeneous field.

Fields that partially cancel can also be generated by opposed solenoids. As shown in Figures IV-9 and IV-10, opposed solenoids can be either aligned or offset. These configurations are analagous to the coil configurations discussed above, and the coordinates used for the two systems are identical.

C. RF Coil Configurations

In addition to the steady magnetic field, an NMR remote detection system must also produce a radio frequency, or rf, field within the region of interest. This rf field must be aligned perpendicular to the steady field in order to produce an NMR response.

Because of practical limitations on the amount of rf power that can be conveniently generated and delivered, it is generally not feasible to use inefficient rf coil configurations (e.g., opposed loops) when short rf pulses are required. A consequence of this constraint is that appropriate rf coil configurations will likely produce an rf field that is inhomogeneous over the useful region of DC field. However, with careful design, it should be possible to minimize the effects of this inhomogeneity.

Three rf coil configurations are examined below. A spiral configuration is discussed first, and this is followed by discussions of the solenoid and semi-toroid configurations.

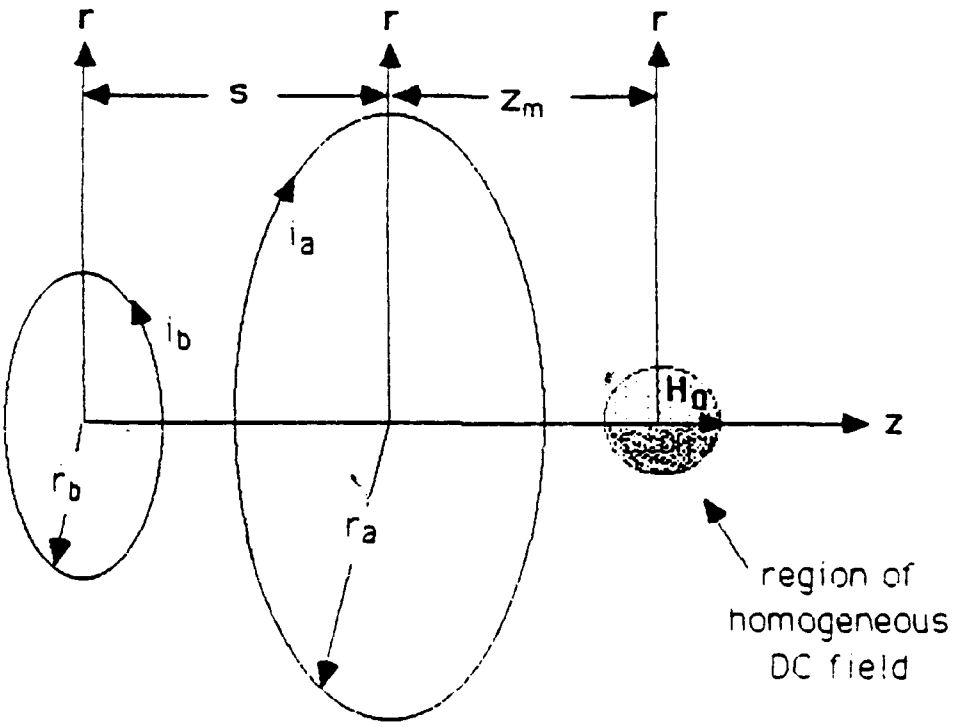

Opposed Coils (Negative Shift)

Figure IV-6

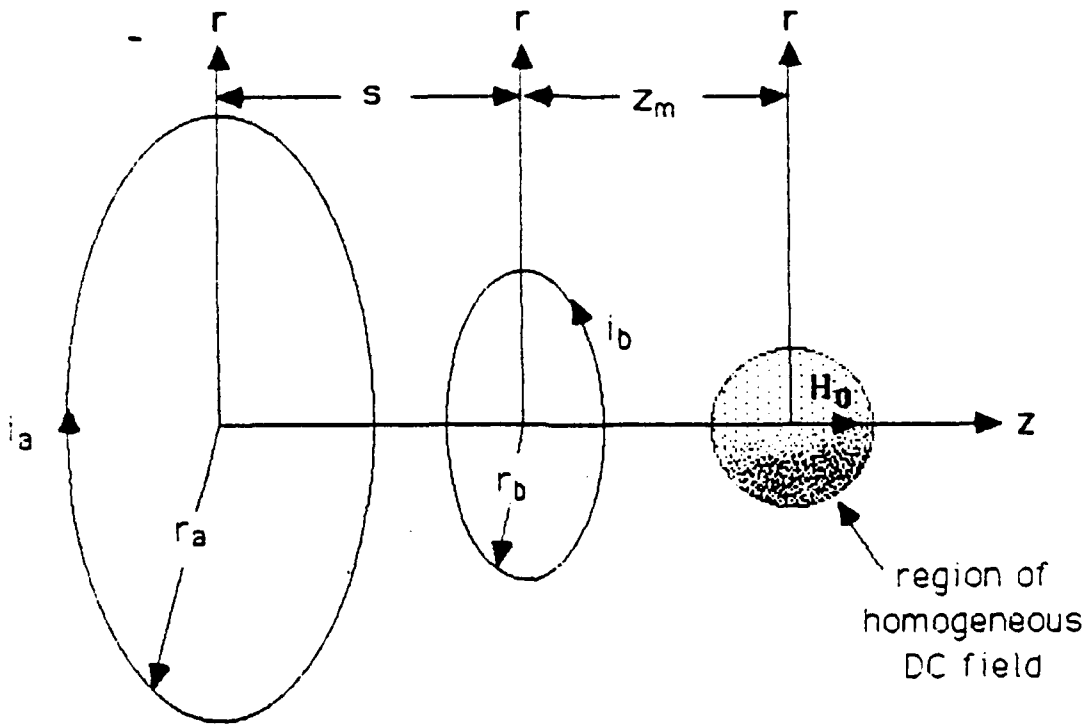

Schematic of Inside-Out Helmholtz Coils
to generate the DC Magnetic Field

Figure IV-7

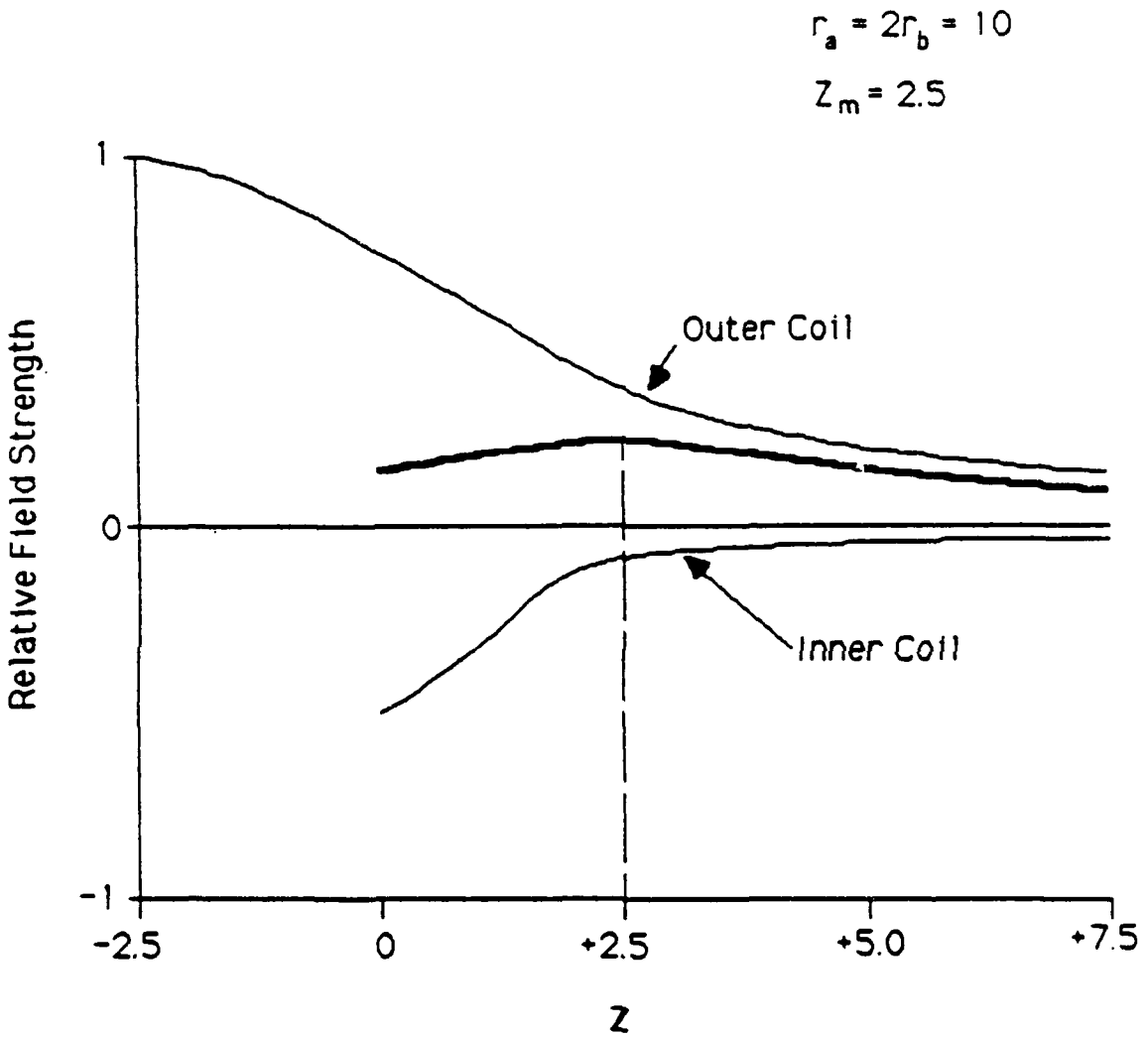

Field Plot for an Inside-Out
Helmholtz Pair

Figure IV-3

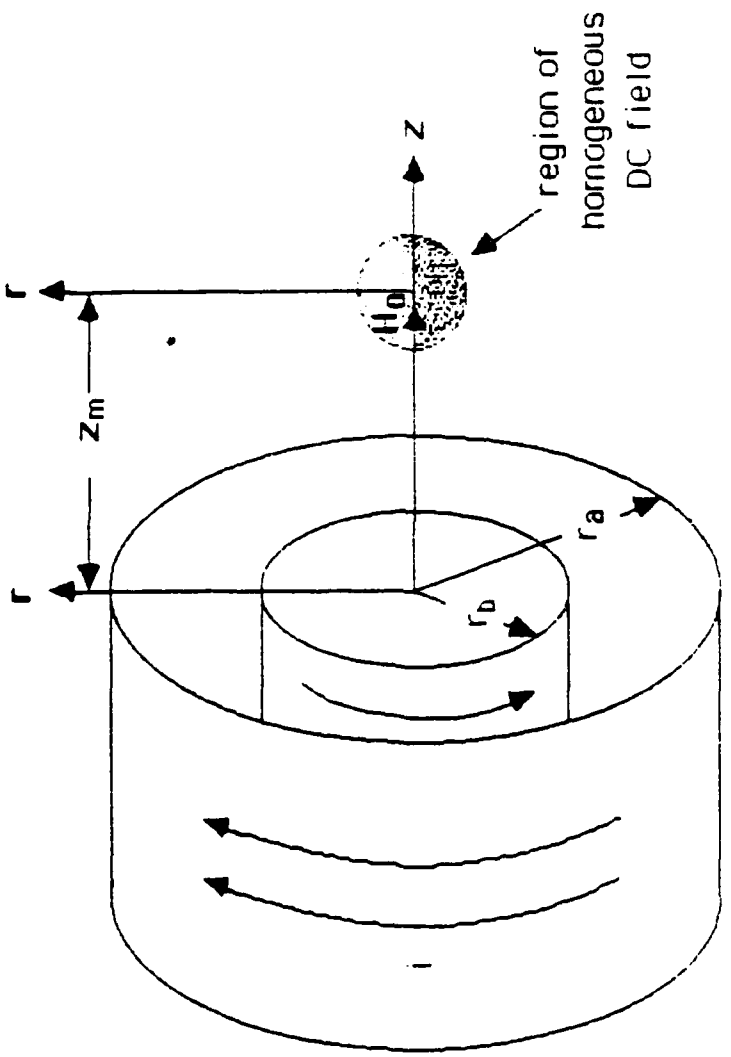

Opposed Solenoids

Figure IV-9

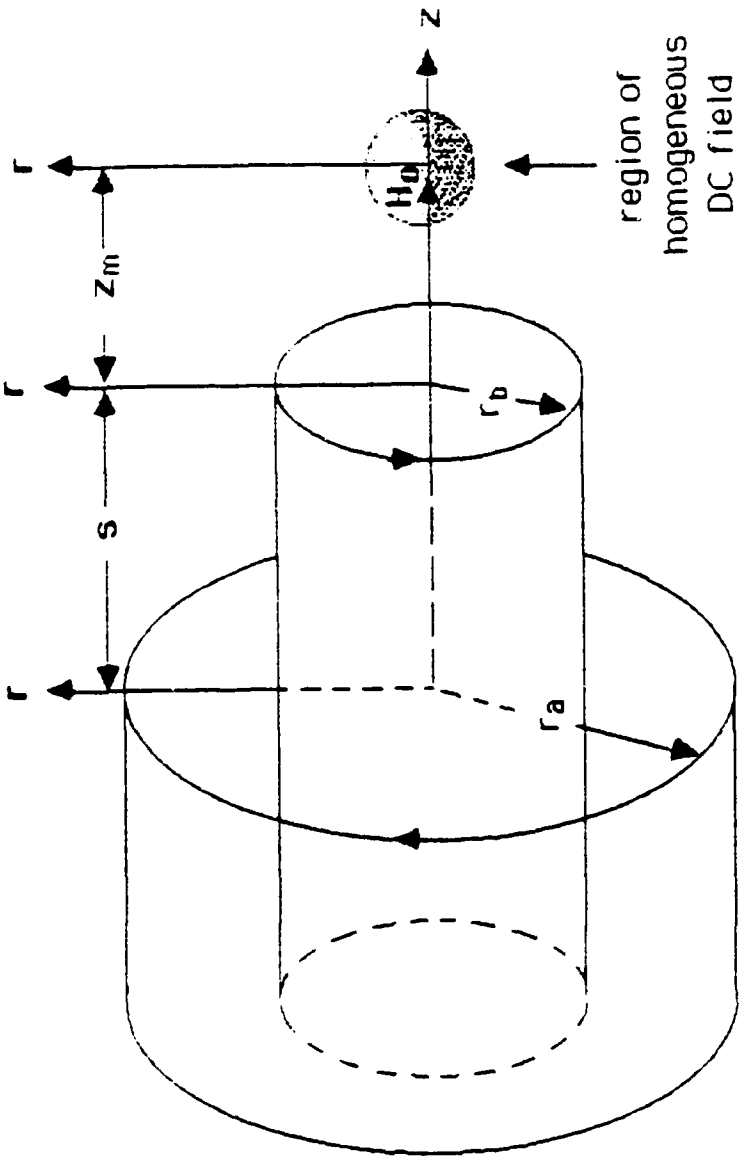

Offset Opposed Solenoids (positive shift)

Figure IV-10

Spiral Coil

The spiral, or spiral-wound, coil is a two dimensional coil which, for analysis, can be considered to be a series of concentric single-turn coils. Spiral coils are sometimes called spiral-wound coils or pancake coils. A spiral coil is shown schematically in Figure IV-11(a).

Near the coil, and along the axis of symmetry, a spiral coil produces a field perpendicular to the plane of the coil winding. This is illustrated in Figure IV-11(b).

For applications as an rf coil in NMR remote detection, the spiral coil must be used in conjunction with a system that produces a DC field perpendicular to the symmetry axis of the spiral coil. Of the systems discussed above, only the U-shaped configuration satisfies this constraint.

There is one obvious drawback to the use of a spiral rf coil in single-sided NMR, which is that the rf field is not focused, or directed, toward the region of interest. If a spiral rf coil is placed flush against the region to be examined, so that the rf field penetrates into the region, then an rf field of equal magnitude is also produced outside the region of interest.

This inefficiency is reflected, in part, by the rf power requirements of the system designed and built to measure moisture levels in structural concrete (3). In this system, an rf pulse power of 200 kilowatts is required to produce a 30 microsecond, 90 degree pulse at a Larmor frequency of 2.1 MHz.

Solenoid Coil

A solenoid coil, which is commonly used in laboratory NMR instruments as the sample coil, is shown schematically in Figure IV-12. From this figure it is obvious that the solenoid coil produces a remote, or fringe, field that in some regions is parallel to the coil axis of symmetry.

The direction of the rf field produced by a solenoid coil makes it appropriate for use with either the toroidal DC field produced by the opposed magnet geometry or the localized DC field produced by opposed loops such as the Inside-Out Helmholtz. It should be pointed out that the symmetry of the field produced by a solenoid coil is ideally suited to the toroidal geometry of opposed magnet NMR. It is less than ideal for use with an Inside-Out Helmholtz geometry since its field pattern is not specifically directed toward the remote region of homogeneous field.

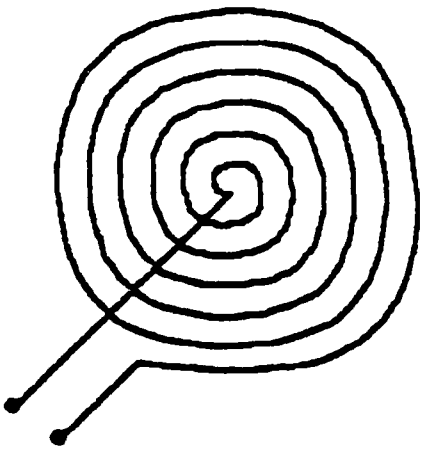

Spiral Coil (Face View)

Figure IV-11(a)

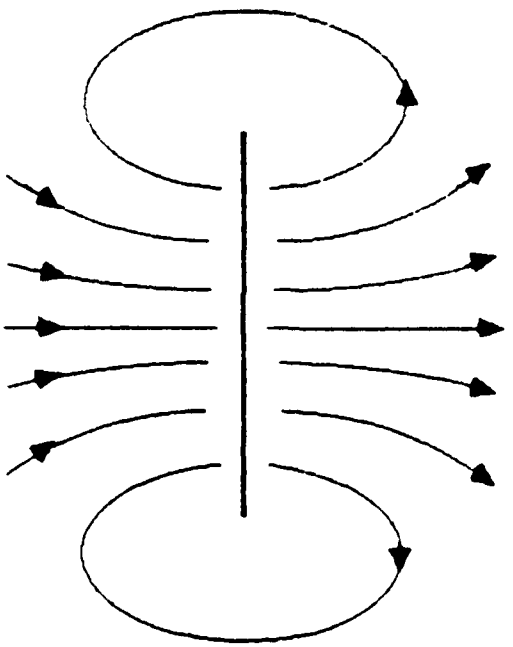

Spiral Coil (Edge View)
with Field Lines

Figure IV-11(b)

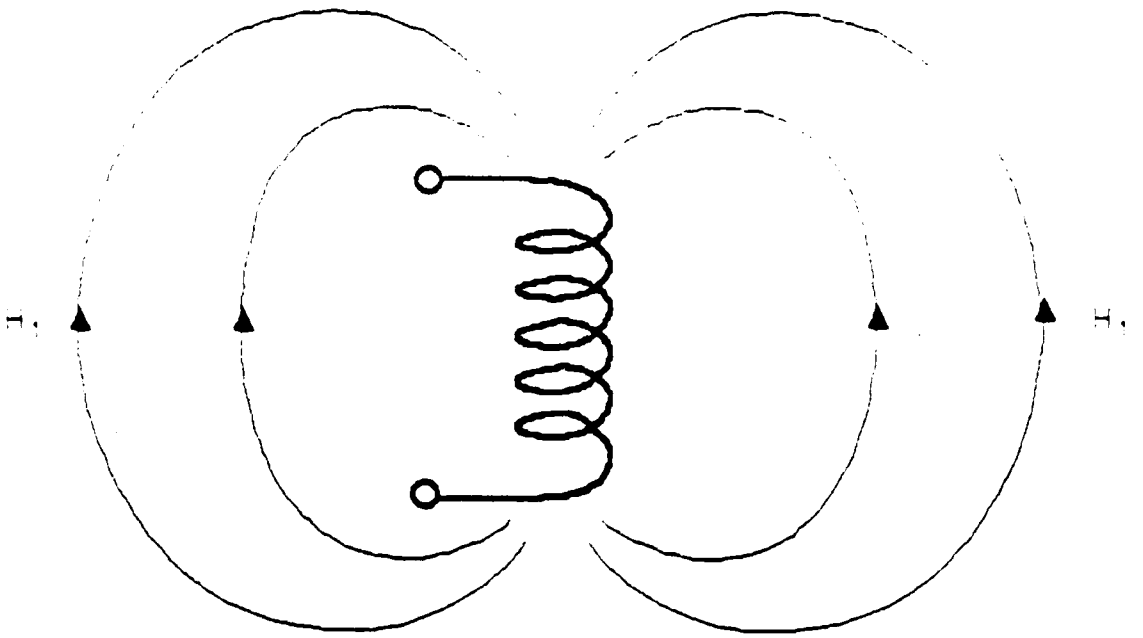

Schematic of Solenoid RF Coil

Figure IV-12

Semitoroid Coil

The semitoroid coil (24) can be thought of in two ways: a) as a solenoid coil which has been bent into a semicircle; or, b) as a donut shaped, or toroidal coil, which has been cut in half. A sketch of a semitoroid coil and its accompanying field lines, is shown in Figure IV-13.

The semitoroid rf coil produces an H1 field which is perpendicular to the axis of symmetry of the coil, i.e., the Z axis. This means that the semitoroid coil is appropriate for use with the Inside-Out Helmholtz configuration for generating the DC field. In addition, the semitoroid coil produces an rf field pattern that is directed toward the remote region of homogeneous field. Therefore, the semitoroid coil should be more efficient in single-sided NMR systems than either spiral or solenoid coils.

Use of the semitoroid coil to produce the rf field has other potential advantages. The design parameters are very flexible and a given coil can be operated over a wide range of frequencies. Field shaping is also possible, since actual coils could subtend major angles greater than, or less than, 180 degrees.

In addition, semitoroids can be constucted to reduce significantly the electric field associated with the rf pulse. This may be important in some of the anticipated applications.

D. Figure-of-Merit

In order to evaluate and compare alternate spectrometer configurations, a figure-of-merit is required. A figure-of-merit allows potentially-interesting geometries to be screened without the necessity of performing detailed calculations for each one.

To arrive at the figure-of-merit, assume that an NMR spectrometer produces a remote region of field and, further, that the center of this remote region is located a distance Zm from the plane of the coils producing the field. The total nuclear magnetization, Mo, within this remote region is proportional to the product of the volume of the remote region, Vm, times the DC field strength, Ho. That is,

$$Mo \propto Vm * Ho \qquad IV - 1$$

The quantity Mo is a measure of the nuclear magnetization, produced by the spectrometer, that is available to be manipulated. In some sense, Mo is a figure-of-merit. However, Mo is not the figure-of-merit needed to identify promising spectrometer configurations for remote detection.

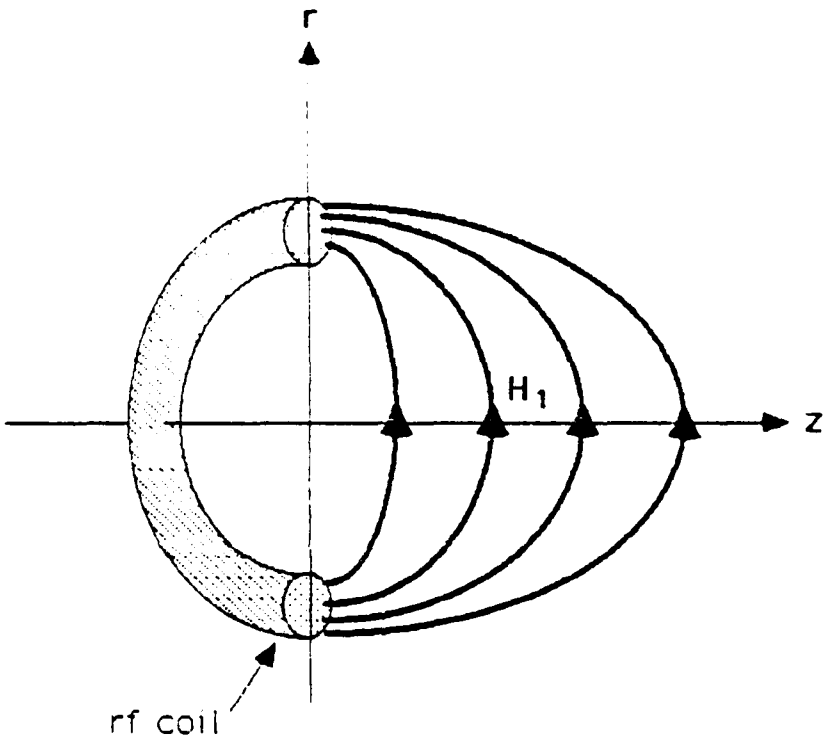

Schematic of Semitoroid RF Coil

Figure IV-13

Following a 90-degree pulse, the voltage, Es, induced in an rf pickup coil located a distance Z away is

$$Es \propto Mo * Wo\ Z^{3} \qquad IV - 2$$

where Wo is the Larmor frequency. Combining (I) and (II), using the fact that Wo is proportional to Ho, and letting Z = Zm allows Fs, the figure-of-merit, to be defined:

$$Fs = Vm * Ho^{2} / Zm^{3} \qquad (IV - 3)$$

Fs is a measure of the NMR signal voltage induced in an rf pickup coil for a given spectrometer configuration. Since the volume of the homogeneous region of field Vm is proportional to Zm cubed (at least to a first approximation, for the cases studied here), and since Ho depends only upon the DC currents applied to the coils, it follows that Fs provides a simple measure for comparing competing configurations.

7. SYSTEM CONFIGURATIONS FOR REMOTE NMR

A. Introduction

Desirable qualities of a single-sided NMR system for remote detection applications include:

* a penetration depth of 15 - 20 cm, or more;
* portability, perhaps with a moveable inspection head; and,
* a well-defined region of homogeneous magnetic field with a strength of at least 1,000 Gauss.

To elaborate, a minimum penetration depth in the range of 15 to 20 cm will be required in many of the anticipated inspection applications. In general, of course, the greater the penetration depth, the better.

In some applications, portability of the resulting system may be required; in others, portability may be very desirable. Transportability, in contrast to portability, will be important in virtually all potential applications.

A field strength of at least 1,000 Gauss will be required for an adequate signal-to-noise ratio and, in addition, for utilizing such potentially-unique NMR signatures as hydrogen/nitrogen level crossing. A well-defined region of homogeneous field will be important in applications where the precise location of the material of interest must be determined.

With these goals in mind, five alternate system configurations for remote NMR detection were considered. These five system configurations are briefly described below.

1. A system utilizing the toroidal geometry of the opposed magnet configuration. In this system, opposing magnets are used to produce the remote region of homogeneous DC field and a solenoid coil is used to produce the rf field.
2. An instrument configuration in which the DC field is produced by a U-shaped iron-core magnet and the rf field is produced by a flat spiral coil.
3. An instrument configuration in which opposed coils or solenoids are used to produce the homogeneous region of DC magnetic field and a semitoroid is used to produce the rf field.

4. A system configuration in which opposed coils or solenoids are used to produce a homogeneous region of rf field, and the required DC field is produced by an alternate configuration, e.g., a semitoroid.

5. An instrument configuration in which both the DC and rf fields are produced by semitoroids and are relatively nonuniform.

Development work has been carried out previously on the first two configurations and the results of this work are described in the next section. This is followed by a discussion of advanced-design single-sided NMR remote detection systems. In the final section of this chapter, the proposed single-sided systems are evaluated using the figure-of-merit developed in Chapter IV.

B. Present Technology

Recent work in remote detection NMR has been directed toward two principal applications. Remote Inside-Out NMR was conceived and developed as a borehole logging tool for geophysical evaluation. Single-sided NMR using a U-shaped magnet was developed for measurements of moisture in structural concrete and subsurface soils. These two technologies are discussed in the following sections.

Inside-Out NMR

Inside-Out NMR was developed for the remote detection of fluids trapped in porous rock formations adjacant to a borehole (5,6,7). An Inside-Out NMR system combines two of the components discussed in Section IV.B: an opposed magnet system (to produce a toroidal region of DC field) and a solenoid coil (to produce a perpendicular rf field in the remote region).

A sketch of an Inside-Out NMR system is shown in Figure V-1 (7). The rf coil is located halfway between, and on the axis of, the two magnets that produce the DC field. The magnetic field in the toroidal region is directed radially outward, and the fringe field of the solenoid rf coil intersects the DC field at a 90 degree angle.

When an rf pulse is applied to the solenoid coil, as shown in Figure V-1, the nuclear magnetization in the remote region is tipped from its equilibrium position. The duration of the rf pulse and the strength of the rf field determine the tip angle.

At the end of the rf pulse, the nuclear magnetization precesses about the steady field, as shown in Figure V-2 [7]. The precessing magnetization induces a voltage across the leads of the solenoid coil, i.e., the NMR free induction decay signal.

Figure V-1

APPLICATION OF 90 ° RF PULSE TO MAGNETIZATION IN HOMOGENEOUS TOROIDAL REGION

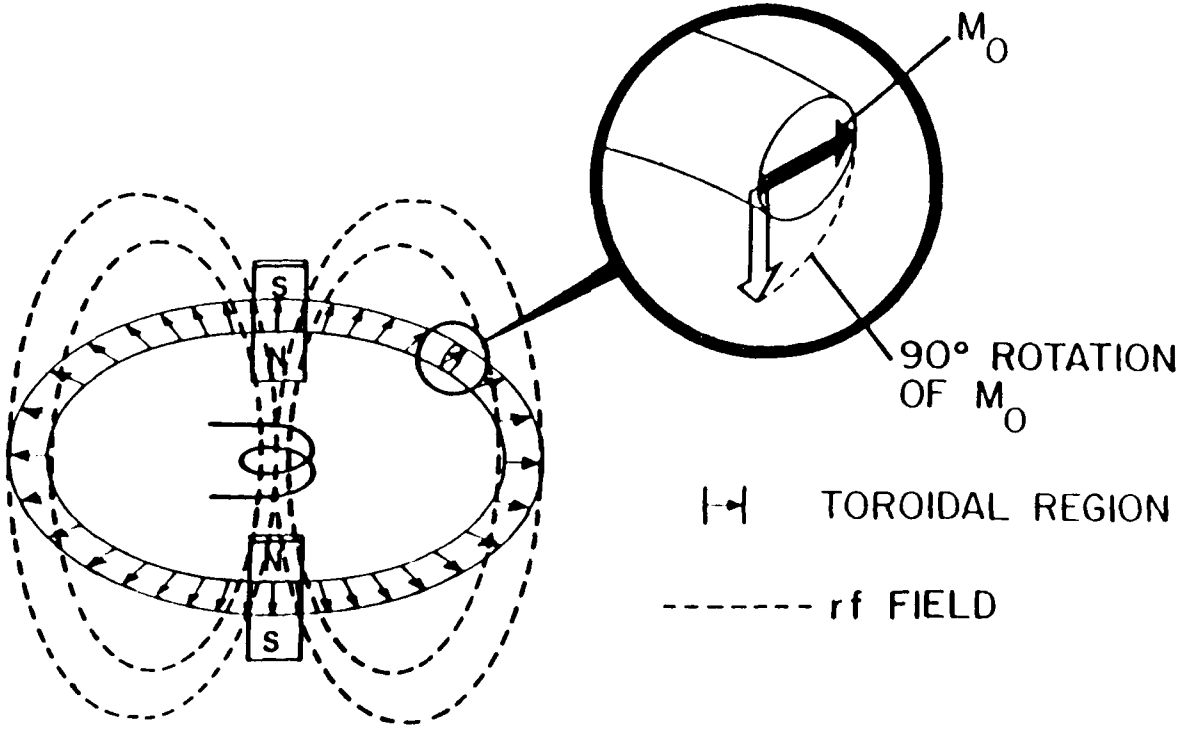

Figure V-2

RECEIVING NMR SIGNAL FOLLOWING 90 ° PULSE.

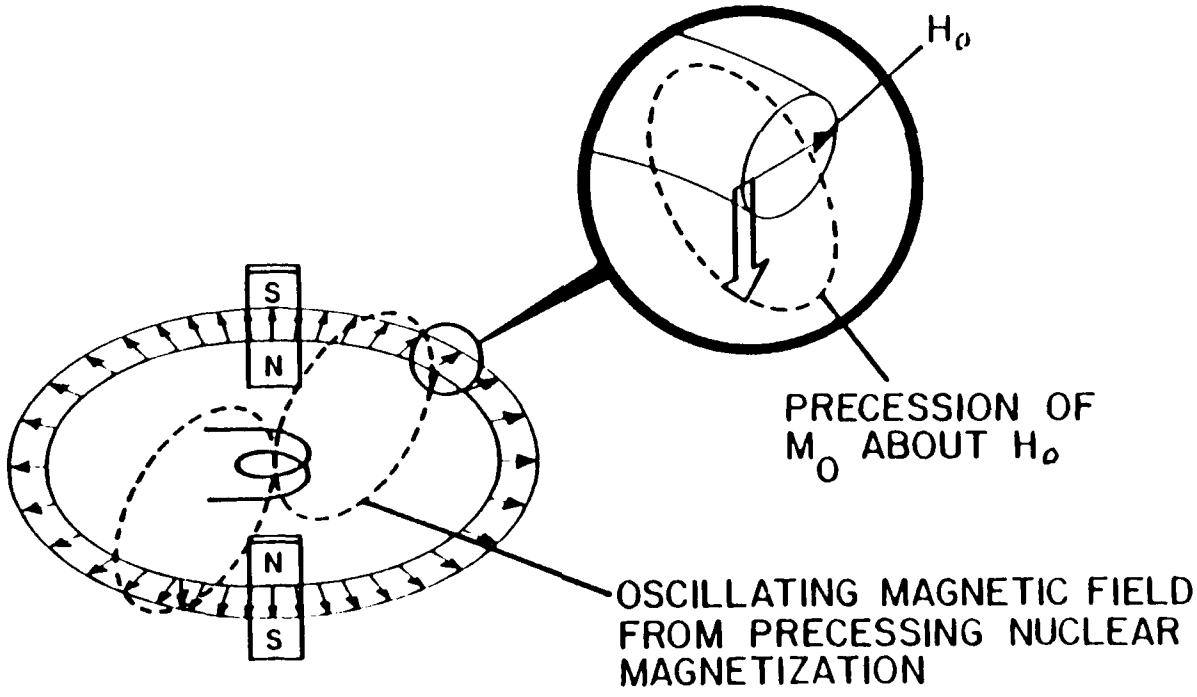

While the geometry of Inside-Out NMR is ideal for remote detection in well logging applications, it is less suitable for those applications where access is limited to only one side. In addition, at the penetration depths required, it is unlikely that the Inside-Out geometry could produce the required field strengths of 1,000 Gauss, even with superconducting coils [8].

Single-Sided NMR

Single-sided NMR systems have been developed in recent years to measure moisture levels in structural concrete and in subsurface soils. Like Inside-Out NMR, discussed above, these systems also utilize two of the components discussed in Section IV.B. First, an electromagnet with a U-shaped yoke is used to produce the DC magnetic field. Then, a spiral rf coil is used for both transmitting the rf pulse and receiving the NMR signal. A sketch of a single-sided system of this type is shown in Figure V-3 [3].

The single-sided NMR system for moisture detection in structural concrete [3,4] employs an iron-core magnet with a U-shaped yoke. The interior length of the U-shaped yoke is 11 inches, the center to center distance between the magnet pole faces is about 15 inches (38 cm), and the system is designed to operate at a field strength of 494 Gauss.

The useable penetration depth of this system is about 10 cm, although the magnet produces 494 Gauss fields at distances of up to 15 cm. Presumably, limitations in the rf components preclude operation at penetration depths between 10 and 15 cm. As configured, the system operates at 2.1 Megahertz and requires 200 kilowatts of rf power to produce a 30 microsecond 90-degree pulse.

At a penetration depth of 2.5 cm, the sensitive region is approximately 7.5 cm in diameter and 0.6 cm thick. As expected, the sensitive volume increases with increasing distance from the instrument.

Single-sided systems designed around iron magnets with U-shaped yokes are, by necessity, quite heavy. The electromagnet for the system described above weighs approximately 600 pounds, and the associated equipment weighs an additional 450 pounds.

C. Advanced Single-Sided NMR Systems

The drawbacks of the Inside-Out NMR geometry for single-sided NMR applications are obvious. Furthermore, it would be difficult, perhaps impossible, to engineer a single-sided NMR system incorporating a U-shaped, iron-core magnet that would exhibit all the desirable qualities discussed in Section A of this chapter.

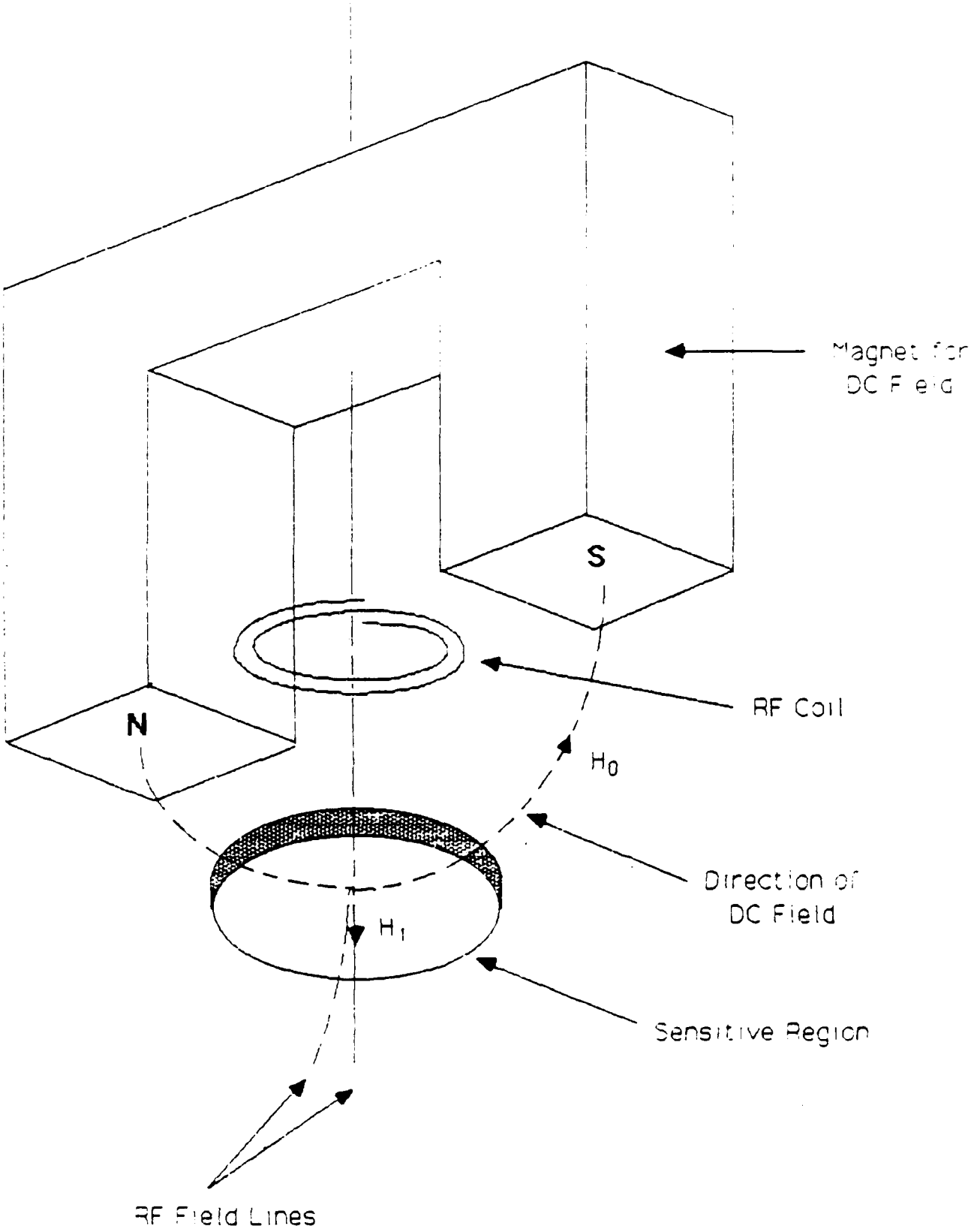

Figure V-3

A Single-Sided NMR System
Utilizing an Iron-Core Electromagnet

Major improvements to present technology are required in three principal areas:

1. The strength of the magnetic field in the remote region must be increased.

2. The penetration depth, or distance to the remote region of homogeneous field, must be increased.

3. The coupling of the rf field to the remote region of homogeneous field must be improved.

To address these issues, three potential single-sided NMR configurations were considered. The first utilizes opposed loops and or solenoids to produce the remote region of DC field and a semitoroid to produce the rf field. This is termed Opposed Loop Semitoroid Remote NMR.

The second utilizes a semitoroid to produce the Ho field and opposed loops or solenoids to produce the remote rf field. This is termed Semitoroid Opposed Loop Remote NMR.

The third utilizes two semitoroid coils, one for the DC field and the other for the rf field. This is termed Double Semitoroid Remote NMR. These three possible system configurations are discussed below.

Opposed Loop/Semitoroid Single-Sided NMR System

An opposed loop/semitoroid single-sided NMR system is shown in Figure V-4. Steady currents flowing through the opposed loops produce the remote region of homogeneous field, Ho, which is directed along the Z-axis. The rf field, H1, is produced by a semitoroid and is directed perpendicular to the Ho field.

An advantage of this configuration is that the homogeneous region of field is large and well-defined. However, a potential drawback is that the rf field may vary significantly over the volume of the Ho field. It is quite likely, though, that field shaping could be used to optimize coupling between the two fields.

Semitoroid Opposed Loop Single-Sided NMR System

A semitoroid opposed loop single-sided NMR system is shown in Figure V-5. The DC field, Ho, is produced by a semitoroid and is directed perpendicular to the Z-axis. The rf currents flowing through the opposed loops produce a homogeneous region of rf field, H1, which is directed along the Z-axis.

Compared to the previous configuration, this system offers few advantages. The rf field is uniform within the region of

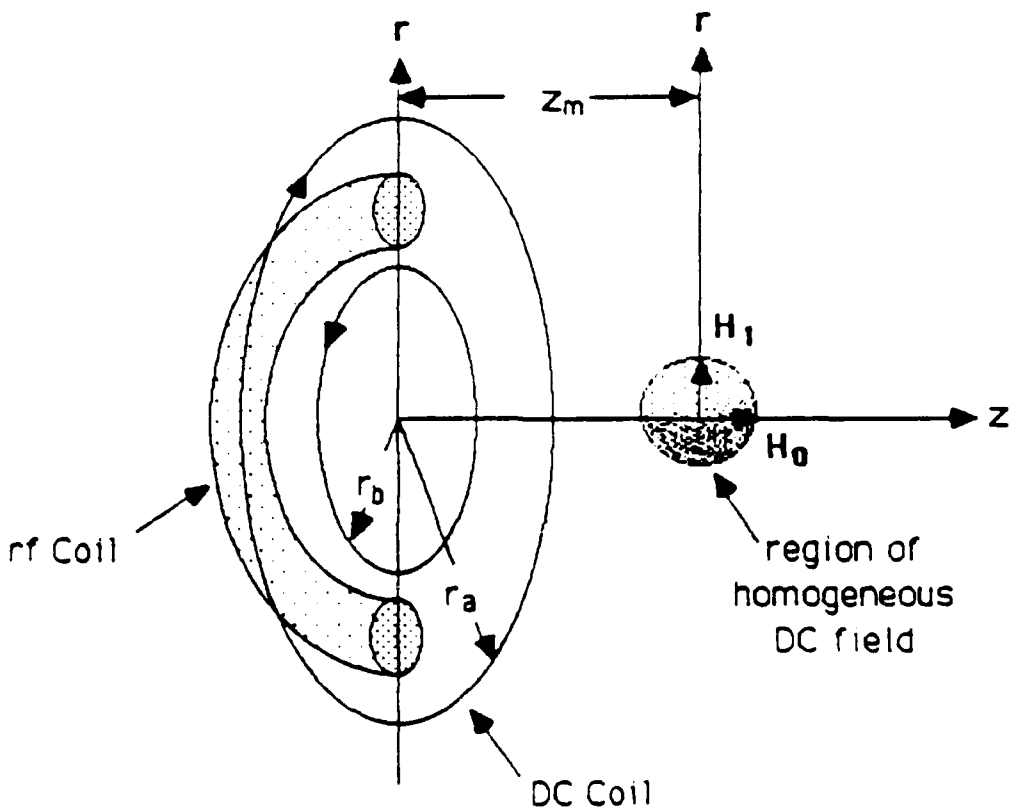

Opposed Loop / Semitoroid
Remote NMR

Figure 7-4

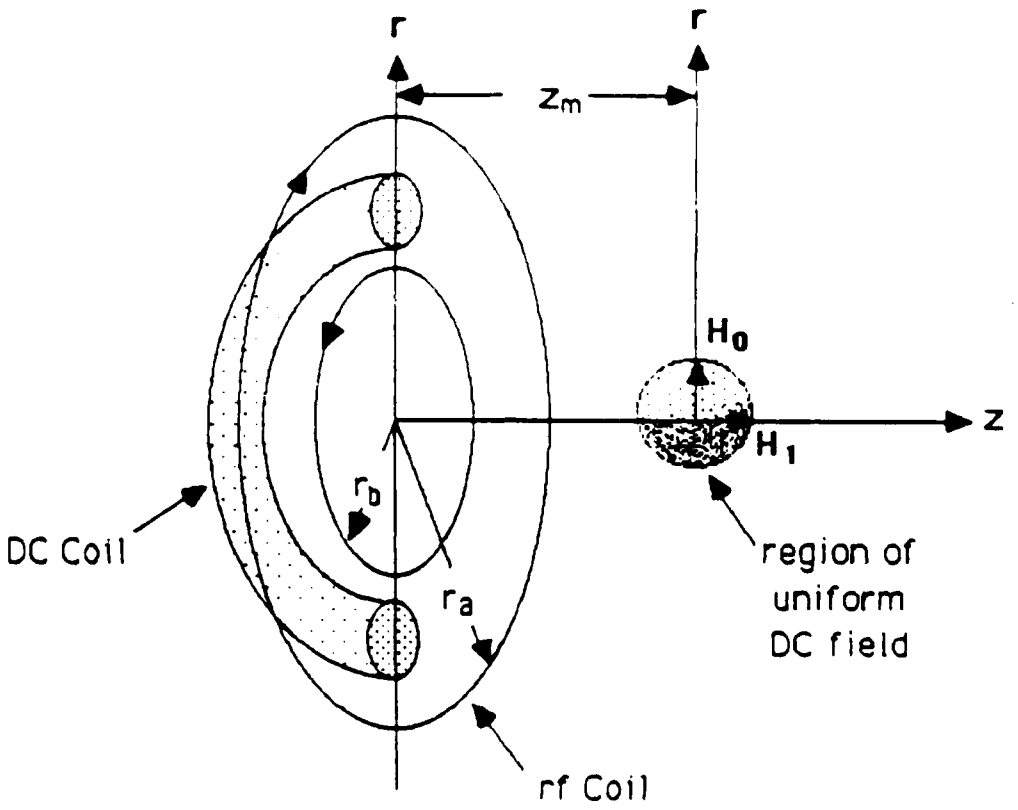

Semitoroid / Opposed Loop
Remote NMR

Figure V-5

interest, but significant, [illegible] field is produced by opposed loops.

In addition, the Ho field in this system is significantly more inhomogeneous. In principle, this allows the region that the NMR signal arises from to be specified more precisely. However, the penalty in signal-to-noise ratio, resulting from a much smaller sample volume, would likely be significant.

Double Semitoroid Single-Sided NMR System

A double semitoroid single-sided NMR system is shown in Figure V-6. Both the DC and rf fields are produced by semitoroid coils. The semitoroids are aligned at 90 degrees to one another and to the Z axis. As a result, the Ho and H1 fields are perpendicular.

An advantage of this configuration is that the rf coil is more efficient that of the semitoroid opposed loop system above. However, the rf coil in this system is identical to that of the opposed loop semitoroid system, and that configuration has the additional advantage of a homogeneous DC field.

D. Evaluation of Alternate Remote NMR Systems

The proposed single-sided NMR systems based upon opposed coils or solenoids to produce the DC field and semitoroid coils to produce the rf field possess clear qualitative advantages over the other potential configurations discussed in the previous section. In order to select the most attractive of the remaining systems, the figure-of-merit, introduced in Chapter IV, was employed.

The figure-of-merit, Fs, was calculated for each of the four possible systems. Since semitoroids are utilized as rf coils, the systems differ in the methods used to produce the DC fields. The DC magnetic fields are produced in four different ways: with opposed solenoids, with opposed offset solenoids, with opposed loops, or with opposed offset loops in the Inside-Out Helmholtz configuration. Each of these cases is discussed in turn below.

The notation used in these discussions is similar to that used by Rath, et al [23]. The diameter of the largest coil or solenoid is assumed to be 10 units. The field produced at the center of this coil or solenoid is assumed to have a magnitude of one. The diameter of the smaller coil or solenoid, the field it produces, and its offset distance (if any) are all adjustable parameters. The effects of inhomogeneity in the rf field are ignored.

Opposed Solenoid Semitoroid System

An analysis of several opposed solenoid configurations is shown in Table V-1. Regarding the column headings, Zm is the point in the Z axis where the maximum in field occurs, Bm is the relative

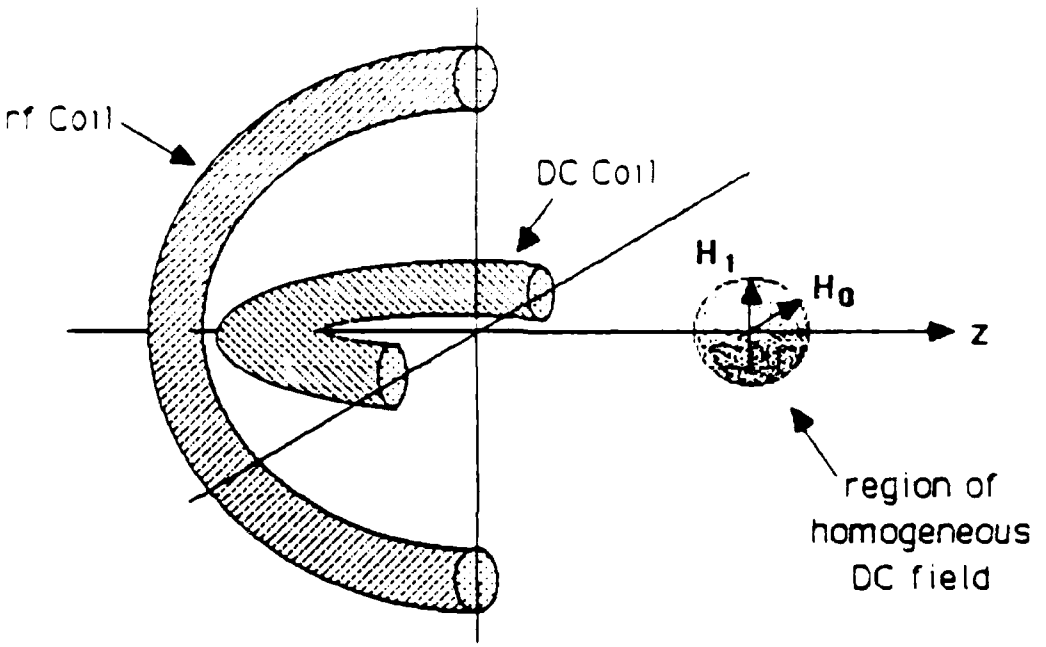

Double Semitoroid
Remote NMR

Figure 7-6

Table V-1

FIGURE-OF-MERIT AND CHARACTERISTICS
OF OPPOSED SOLENOIDS

The diameter of the outer solenoid Ra = 1.0 units, and the magnitude of the field at the center of this solenoid is a = 1.0. The diameter of the inner solenoid is Rb, and the magnitude of the field at the center of this solenoid is b. The outer and inner solenoids are each 1.0 units long, and the offset distance is zero.

The point of maximum field on the Z axis is Zm. The field strength at Zm is Bm. The diameter of the homogeneous region, defined by a 100 ppm change in B, is dZ and the volume of this region is Vm. No is the nuclear magnetization, and Fs is the figure-of-merit. Notations of the form x E+Y mean "times ten raised to the Y-th power".

Rb	b	Zm	Bm	dZ	Vm xE+4	No xE+4	Fs xE+4
1	1.0	0.724	0.410	0.103	5.72	2.44	208.
2	1.5	4.844	0.158	0.106	6.24	2.11	92.4
3	2.0	5.795	0.074	0.110	6.87	1.91	24.9
5	3.0	4.434	0.260	0.126	10.47	2.72	14.4
7	4.0	7.510	0.148	0.132	12.04	2.78	9.2
9	5.0	10.133	0.092	0.146	16.10	3.14	7.5

magnitude of the field maximum, and dC is the diameter of the remote region. In these examples, the remote region is defined by a field homogeneity of 100 parts per million and, for simplicity, is assumed to be spherical.

The quantity Vm is the volume of the remote region, and Mo is a quantity related to the magnitude of the induced nuclear magnetization within the remote region. The quantity Fs is the figure-of-merit defined in Section IV.D.

Several facts are immediately obvious from Table V-1. First, as the current in the small-diameter solenoid increases (i.e., as "b" increases), the distance to the remote region (Rm) increases and the magnitude of the remote field (Bm) decreases. Also, as the diameter of the smaller solenoid increases, the distance to the remote region increases and the magnitude of the remote field decreases.

However, the most interesting observation is that the figure-of-merit, Fs, decreases when the diameter of the smaller solenoid increases, and also when the current flowing through the smaller solenoid increases. The calculated values of Fs are compared to other configurations in the sections below.

Opposed Loop/Semitoroid System

Similar calculations for an opposed loop/semitoroid system are presented in Table V-2. There are a number of similarities between the opposed loop and opposed solenoid systems, including the expected dependences on the inner coil diameter and current.

The most interesting result, however, and certainly the most important, is that there appears to be little or no advantage in utilizing solenoids over loop in a single-sided remote NMR system. When the inner loop is operated at lower currents, the figures-of-merit are comparable to those of the opposed solenoid system. At higher currents, larger values of Fs are obtained for the opposed loop system.

Offset Opposed Solenoid Semitoroid System

The figure-of-merit was calculated for a series of offset opposed solenoids. These solenoids were assumed to be semi-infinite, with a diameter of 10 for the outer solenoid and 5 for the inner. Each was assumed to produce a field of unity magnitude at the origin. The results are presented in Table V-3.

The offsets range from -2.5 units to +2.5 units. A positive offset means that the outer solenoid is moved back, in the negative Z direction, by a distance d, the amount of the offset.

Offsetting the two solenoids results in dramatic changes in the system figure-of-merit. For example, with zero offset, the

Table V-2

FIGURE-OF-MERIT AND CHARACTERISTICS
OF OPPOSED LOOPS

The diameter of the outer loop is Ra = 1.0 units, and the magnitude of the field at the center of this loop is a = 1.0. The diameter of the inner loop is Rb, and the magnitude of the field at the center of the inner loop is b. The offset distance is zero.

The point of maximum field on the Z axis is Zm. The field strength at Zm is Bm. The diameter of the homogeneous region, defined by a 100 ppm change in B, is dZ and the volume of this region is Vm. Mo is the nuclear magnetization, and Fs is the figure-of-merit. Notations of the form x E+Y mean " times ten raised to the Y-th power".

Rb	b	Zm	Bm	dZ	Vm xE+4	Mo xE+4	Fs xE+8
0	1.0	4.07	0.388	0.097	4.78	2.81	188.
0	1.5	5.09	0.511	0.095	4.49	2.29	88.9
0	2.0	5.67	0.454	0.095	4.49	2.04	60.8
0	4.0	6.73	0.369	0.111	7.36	2.72	50.3
0	1.5	7.32	0.256	0.109	6.78	1.74	11.3
0	2.0	8.73	0.182	0.111	7.36	1.34	3.66

Table V-3

FIGURE-OF-MERIT AND CHARACTERISTICS
OF OFFSET OPPOSED SOLENOIDS

The diameter of the outer solenoid Ra = 10 units, and the magnitude of the field at the center of this solenoid is a = 1.0. The diameter of the inner solenoid is Rb = 5 units, and the magnitude of the field at the center of this solenoid is b = 1.0. The outer and inner solenoids are semi-infinite; the offset distance is given by S.

The point of maximum field on the Z axis is Zm. The field strength at Zm is Bm. The diameter of the homogeneous region, defined by a 100 ppm change in B, is dZ and the volume of this region is Vm. Mo is the nuclear magnetization, and Fs is the figure-of-merit. Notations of the form x(E+Y) mean "times ten raised to the Y-th power".

S	Zm	Bm	dZ	Vm (xE-4)	Mo (xE+4)	Fs xE-6
-2.5	1.438	0.476	0.125	10.2	4.86	[illegible]0.
-2.0	2.042	0.428	0.124	9.98	4.27	2150.
-1.5	2.690	0.382	0.124	9.98	3.81	748.
-1.0	3.386	0.338	0.124	9.98	3.37	294.
-0.5	4.133	0.298	0.124	9.98	2.97	126.
0	4.934	0.260	0.126	10.5	2.72	58.9
0.5	5.291	0.226	0.128	11.0	2.49	37.9
1.0	5.702	0.196	0.130	11.5	2.25	23.8
1.5	6.164	0.168	0.134	12.6	2.12	15.2
2.0	6.674	0.146	0.138	13.3	2.01	9.90
2.5	7.729	0.126	0.144	15.6	1.97	6.56

calculated value of Fs is 58.9 x (E-8). As the offset is increased to S = +2.5, Fs falls to 6.56 x (E-8), almost a factor of ten.

However, when the solenoids are offset in the opposite direction to S = -2.5, Fs increases to 7.7 x (E-5). This represents an increase of over a factor of 100. The latter value of Fs represents a significant improvement over any of the previous configurations.

Inside-Out Helmholtz/Semitoroid System

Calculations of Fs and other relevant parameters for Inside-Out Helmholtz/Semitoroid systems are presented in Table V-4. Although the maximum attainable field strengths for these systems are comparable to those of the previous configurations, the remote regions of homogeneous field are much larger. This leads to a direct increase in the figure-of-merit.

For example, with an inner coil diameter of five, a set of simple opposed loops gives Fs = 53.3 x (E-8). The comparable value for an Inside-Out Helmholtz configuration is Fs = 22.5 x (E-5), which is over a factor of 400 larger. In addition, this Fs is almost a factor of three larger than the most favorable configuration of offset opposed solenoids.

The figure-of-merit is a strong function of the diameter of the inner coil, and as this diameter increases, Fs decreases. However, both the overall size of the coil system and the penetration depth increase with increasing inner coil diameter, so practical considerations may lead to compromises in the choice of system configuration.

Table V-4

FIGURE-OF-MERIT AND CHARACTERISTICS
OF INSIDE-OUT HELMHOLTZ OPPOSED COILS

The diameter of the outer coil is Ra = 10 units, and the magnitude of the field at the center of this coil is a = 1.0. The diameter of the inner coil is Rb, and the magnitude of the field at the center of the inner coil is b. The offset distance is S.

The point of maximum field on the Z axis is Zm. The field strength at Zm is Bm. The diameter of the homogeneous region, defined by a 100 ppm change in B, is dZ and the volume of this region is Vm. Mo is the nuclear magnetization, and Fs is the figure-of-merit. Notations of the form x(E+Y) mean "times ten raised to the Y-th power".

Rb	b	S	Zm	Bm	dZ	Vm (xE+2)	Mo (xE-3)	Fs (xE-5)
3	0.3	3.5	1.5	0.501	0.279	1.14	5.71	84.8
4	0.4	3.0	2.0	0.429	0.330	1.88	8.07	43.2
5	0.5	2.5	2.5	0.358	0.374	2.74	9.81	22.5
6	0.6	2.0	3.0	0.286	0.413	3.69	10.6	11.2
7	0.7	1.5	3.5	0.215	0.448	4.71	10.1	5.08
8	0.8	1.0	4.0	0.143	0.481	5.83	8.33	1.86

VI. ADVANCED SINGLE-SIDED REMOTE DETECTION NMR SYSTEM

A. Introduction

The figure-of-merit evaluations of the previous chapter lead directly to a preferred configuration for an advanced single-sided NMR system for remote detection applications. Specific features of the preferred configuration, estimated signal-to-noise ratios, and practical considerations associated with implementation are discussed in this chapter.

B. System Configuration

Based upon the figure-of-merit calculations, it appears that a single-sided remote NMR system that utilizes Inside-Out Helmholtz coils to produce the steady Ho field possesses clear advantages over competing configurations. With proper design, such a system should exhibit all or most of the desirable attributes discussed in the previous chapter, i.e., a reasonable penetration depth, portability or transportability, and a well-defined remote region of inspection.

A sketch of the proposed system is shown in Figure VI-1. In this sketch, the semitoroid is shown with a major diameter approximately equal to the diameter of the inner coil of the Inside-Out Helmholtz pair. The optimum configuration would, of course, depend upon the particular choice of Inside-Out Helmholtz geometry. However, assuming Ra = 2(Rb), the configuration illustrated would provide an rf field strength at the center of the remote region approximately 20 - 25% of the field strength available at the semitoroid face. In addition, the inhomogeneity of the rf field over the remote volume is estimated to be less than 10%, which is very attractive.

It may be desirable to design the system with two separate rf coils, one for transmitting and the other for receiving. Such a design may lead to a more efficient use of transmitter power or to an improvement in the signal-to-noise ratio through reduced system recovery time, improved detector coil Q, or the like.

If separate receiver and transmitter coils are required, a simple solution would be to incorporate a solenoid detector coil as shown in Figure VI-2. The detector coil would then be oriented to minimize coupling with the semitoroid. An attractive alternative may be to employ crossed semitoroids similar to those shown in Figure V-6 (24).

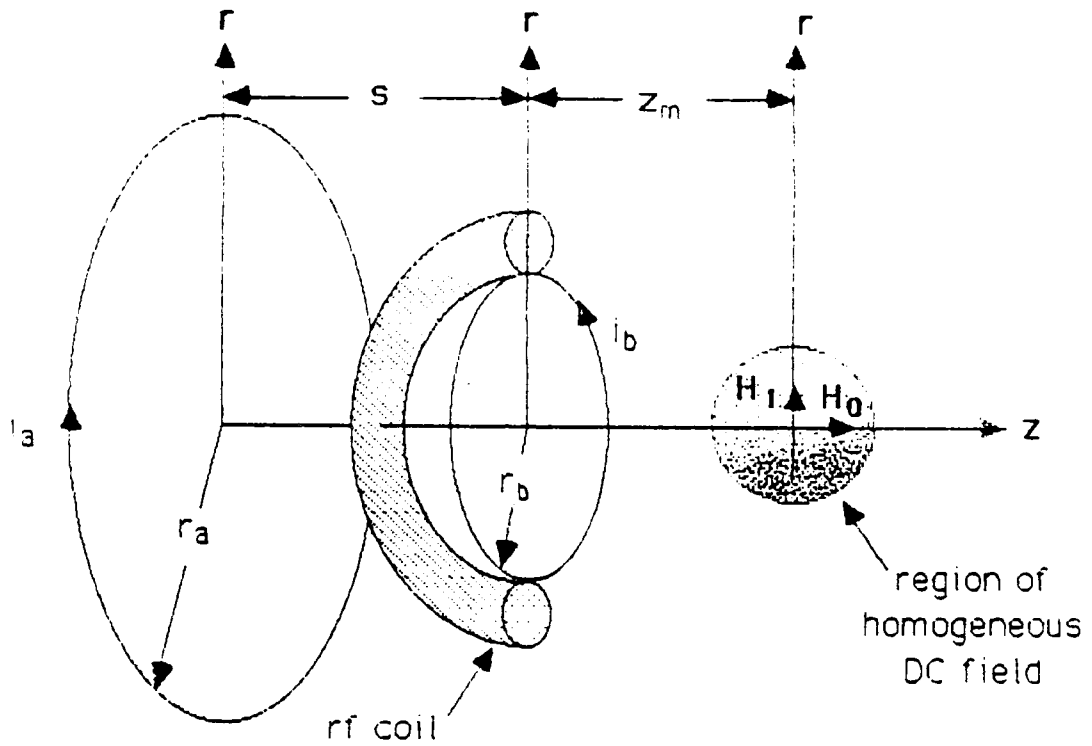

Schematic of Single-Sided NMR System
Utilizing Inside-Out Helmholtz Coils
for the DC Magnetic Field

Figure VI-1

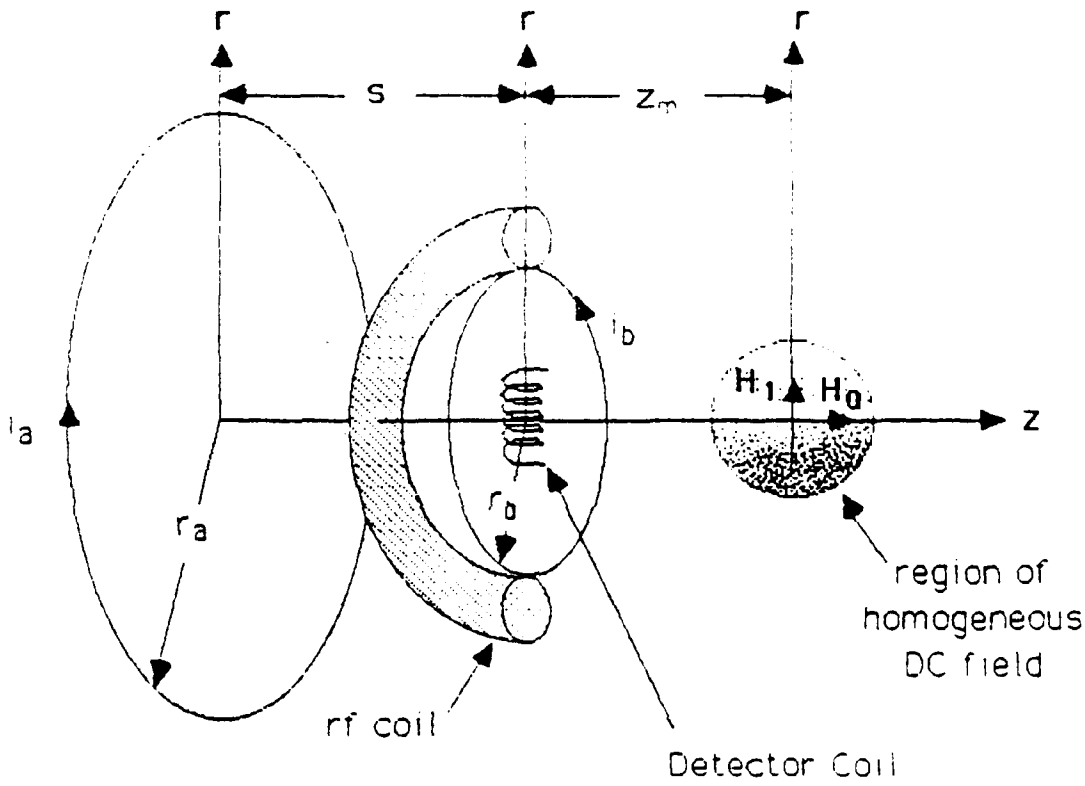

Schematic of Single-Sided NMR System
Utilizing Inside-Out Helmholtz Coils
for the DC Magnetic Field

Figure VI-2

C. Signal-To-Noise Ratio

Equation II-7 was used to calculate the signal-to-noise ratio expected to be observed from a single-sided NMR system producing a 1,000 Gauss field in a remote region 10 centimeters away. Under the following conditions,

Proton Density = 6.6×10^{22};

Sample Temperature = 300 Kelvin;

System Bandwidth, B = 42.57 KHz;

Ra = 2(Rb) = 40 centimeters

d = Zm; Z = 3Zm/2; $\ell/d = 0.5$;

and with the factor F set equal to unity, the SNR was calculated to be

SNR = 11.4.

Although there are a number of effects that will act to reduce the expected SNR from the calculated value, this is an encouraging result. In addition, it is likely that the above conditions could be optimized to produce an even greater estimated SNR.

An interesting result, which arises from the geometry of the Inside-Out Helmholtz system, is that the estimated SNR for a particular configuration is independent of the penetration depth. That is, if the size of the above system is doubled, and the Ho field in the remote region remains the same, then the predicted SNR is again 11.4. The reason is that the volume of the remote region varies as the cube of the penetration depth. Therefore, at constant Ho field, the signal-to-noise ratio is independent of penetration depth. Of course, practical constraints on coil size, rf field strength and the like, make it very unlikely that the SNR would be penetration depth independent, and these effects are addressed below.

It should also be noted that there are effects which will act to reduce the signal-to-noise ratio calculated above. First, the SNR depends directly upon the proton density, and a material with a high proton density was assumed. However, many explosive compounds also have high proton densities, so this may not pose a serious problem.

Second, the SNR calculated above assumes that F = 1.0. The quantity F is a factor that includes the effects of finite rf pulse length, rf field inhomogeneity, system recovery time and signal loss due to short T2 times. Small changes in rf pulse

length or system recovery time can lead to substantial [illegible] in the observed SNR. Since most explosive compounds exhibit short T2 times, these effects are likely to be significant.

It would be difficult to determine the factor F quantitatively, but qualitative estimates are fairly straightforward. F is likely to be a weakly-varying function of penetration depth for small Z and a strongly-varying function of penetration depth for large Z. A reasonable assumption, based upon experience with Inside-Out NMR systems (7,25), is that

$$F \propto Z^{-2}, \text{ for } Z << Zo;$$

$$F \propto Z^{-4}, \text{ for } Z >> Zo;$$

where Zo is a characteristic distance denoting the change in regions.

An analysis of the electrical and physical characteristics of the rf coil in the system above shows that the Q and inductance requirements can be met for coil diameters between about 1 and 27 centimeters. While the lower limit does not present a serious constraint, the upper limit suggests that the transition region occurs near Zo = 27 cm.

The system recovery time depends, to some extent, upon the Larmor frequency, or static field, chosen for observation. The higher the frequency or field, in general, the shorter the recovery time. In addition, the shorter the T2 of the material under study, the greater the loss of signal during the recovery time.

These considerations were collected into the following ad hoc expression for the factor F,

$$F = D * \exp(-1/Ho)/((Z/Zo)^2 + (Z/Zo)^4), \quad (VI - 1)$$

where D and Zo are constants and Ho is the applied field in kilogauss. Since the T2 times of most explosive compounds are similar, and short, the dependence of F on T2 was not explicitly included. Implicit in this expression is the assumption that the effect of the recovery time will reduce the available SNR by a factor of (1/e) at a field of 1,000 Gauss, and more at lower fields.

The effects of rf field inhomogeneity and coupling inefficiencies were then assumed to further reduce the SNR by a factor of two at a field of 1,000 Gauss and a penetration depth of 10 cm. The factor F was then evaluated under the conservative assumption, Zo = 20 cm.

With the inclusion of these numerical values, Equation VI-1 becomes:

$$F = 58.0 * \exp(-1/Ho) * (Z^2(1 - Z^2/625)), \quad (VI - 2)$$

where again Ho is the applied field in kilogauss.

Equations II-7 and VI-2 were used to estimate signal-to-noise ratios for a variety of penetration depths and applied fields. The results are presented in Table VI-1, and the strong dependence of SNR on applied field is immediately obvious. At 0.5 kilogauss, a penetration depth of 2 cm provides a barely adequate SNR, while at 1.5 kilogauss, penetration depths of 50 cm appear feasible.

The SNR also depends strongly upon the configuration of the Inside-Out Helmholtz coils. Predicted signal-to-noise ratios for a variety of configurations are presented in Table VI-2. Two cases are covered in this table. In the first, the Ho fields in the remote regions are assumed to vary as indicated in Table V-4, with a 1,000 Gauss field for the Ra = 40 cm system. In the second, a 1,000 Gauss field is assumed for all configurations.

It is obvious from Table VI-2 that the SNR is strongly dependent upon the system configuration. Unfortunately, the most attractive configurations, from a practical standpoint, also exhibit the lowest signal-to-noise ratios.

Table VI-1

SINGLE-SIDED NMR SIGNAL-TO-NOISE RATIO
VERSUS PENETRATION DEPTH AND APPLIED FIELD

Signal-to-noise ratios for single-sided remote detection NMR systems as a function of the penetration depth in centimeters and the static field in kilogauss. An Inside-Out Helmholtz geometry with Ra = 2 Rb is assumed.

	SIGNAL-TO-NOISE RATIO		
Zm (cm)	0.5 KG	1.0 KG	1.5 KG
2	0.497	5.40	17.0
5	0.304	3.30	10.4
10	0.193	2.09	6.58
20	0.096	1.05	3.29
30	0.053	0.575	1.81
40	0.031	0.341	1.07
50	0.020	0.217	0.682
60	0.014	0.147	0.461

Table VI-1

SINGLE-SIDED NMR SIGNAL-TO-NOISE RATIO
VERSUS COIL CONFIGURATION

Signal-to-noise ratios in single-sided NMR systems employing Inside-Out Helmholtz coils. As indicated below, the penetration depth is 10 centimeters, and the diameter of the inner coil (Rb) is 20 centimeters. The diameter of the outer coil varies depending upon the particular Inside-Out Helmholtz configuration chosen.

Signal-to-noise ratios are presented for two separate cases, A and B). The signal-to-noise ratios presented in column five, Case A, assume that the ampere-turns in the large diameter outer coil is held constant, independent of configuration, and that the field strength in the remote region varies as indicated in Table V-4. Furthermore, for Ra = 40 centimeters, the static field is assumed to be 1,000 Gauss.

The signal-to-noise ratios presented in column six, Case B, assume that the field strength in the remote region is independent of configuration. A field of 1,000 Gauss is assumed for each case.

Ra	Rb	Zm	Ho	SNR (A)	SNR (B)
66.7	20.0	10.0	1.40	10.5	4.02
50.0	20.0	10.0	1.30	4.74	2.79
40.0	20.0	10.0	1.00	2.09	2.09
33.3	20.0	10.0	0.799	0.809	1.63
28.6	20.0	10.0	0.601	0.242	1.31
25.0	20.0	10.0	0.399	0.038	1.08

D. Practical Considerations

In order to implement the proposed single-sided NMR system, a number of practical considerations must be addressed. In particular, the currents required to produce the steady field, the physical advantages and limitations of specific coil geometries, and any electrical electronic limitations must be taken into account. These topics are discussed in the three sections which follow below.

Current Requirements

The required number of ampere-turns to produce a given field strength in the remote region was calculated for several Inside-Out Helmholtz coil geometries. The results for one particular geometry, i.e., the Ra = 2(Rb) geometry, are shown in Figure VI-3. This is a plot of the ampere-turns required in the large diameter coil as a function of the penetration depth, Zm, and the field strength in the remote region, Ho. It can be seen that well over 100,000 ampere-turns are required to produce a remote field of 1,000 Gauss at a distance of 10 cm.

The required number of ampere-turns depends upon the specific geometry of the Inside-Out Helmholtz pair. For constant penetration depth and remote region field strength, the required number of ampere-turns in the outer coil is a minimum for the Ra = 2(Rb) geometry. This is shown in Figure VI-4, which assumes an outer coil diameter Ra = 10 units.

The required number of ampere-turns for the inner coil of the Inside-Out Helmholtz pair is shown in Figure VI-5. The calculations for this plot also assume an outer coil diameter of 10.

From the results shown in Figures VI-3, VI-4 and VI-5, it is obvious that it would be very difficult, and likely impossible, to produce substantial fields at significant penetration depths using conventional resistive coil technology. Pulsed fields could be used in certain applications, but the resulting system would likely be quite complex, especially since explosives tend to exhibit long T1 times.

Employing superconducting coils may be an attractive solution to this problem since it is likely that superconducting coils could produce useable remote field strengths and penetration depths. Of course, there are drawbacks to the use of superconducting coils, but these drawbacks could be overcome in many potential applications. Several important considerations involved with the use of superconducting coils are discussed under the section entitled "Coil Limitations" below.

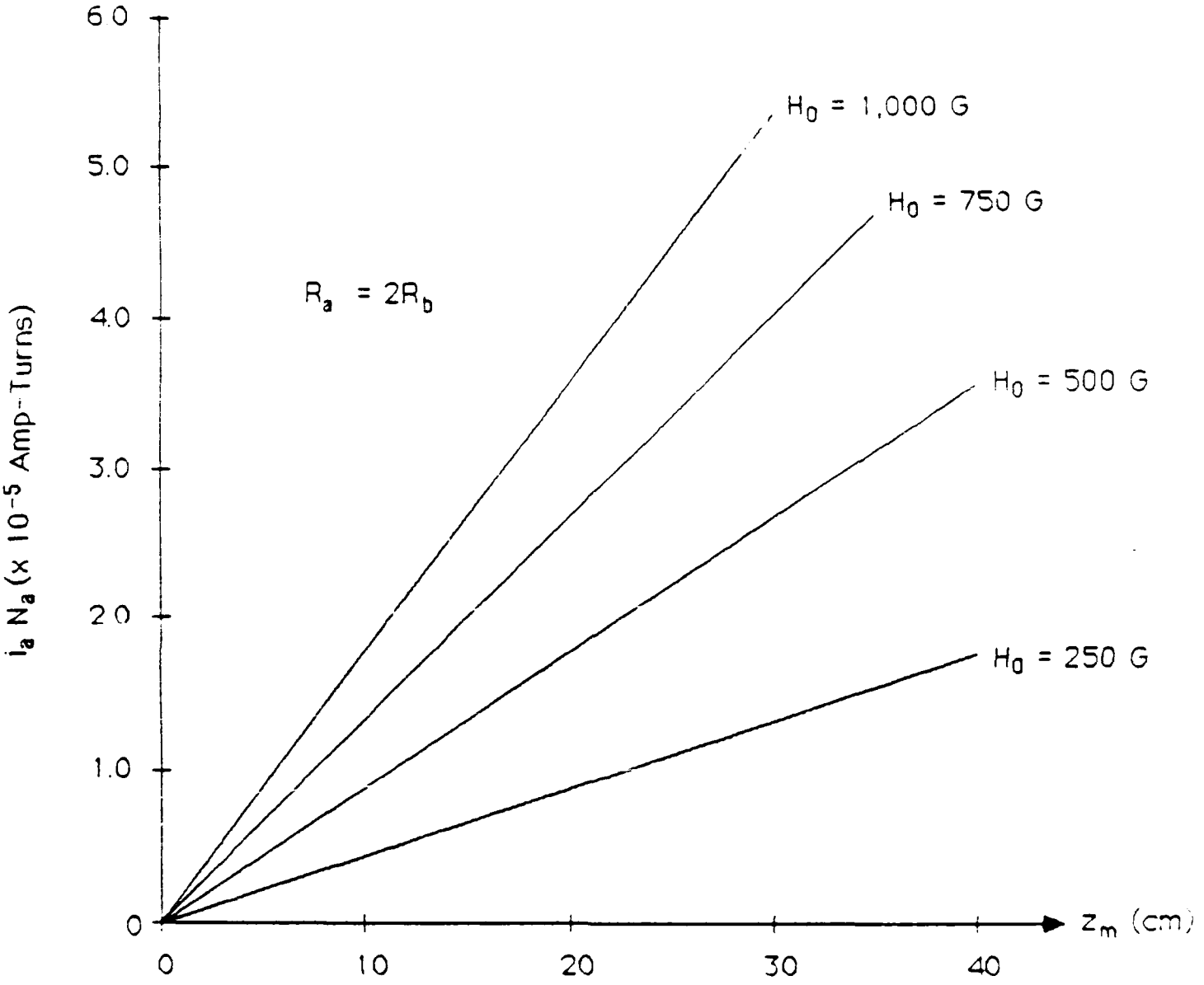

Outer Coil Ampere-Turns versus
Penetration Depth and Remote Field

Figure [illegible]

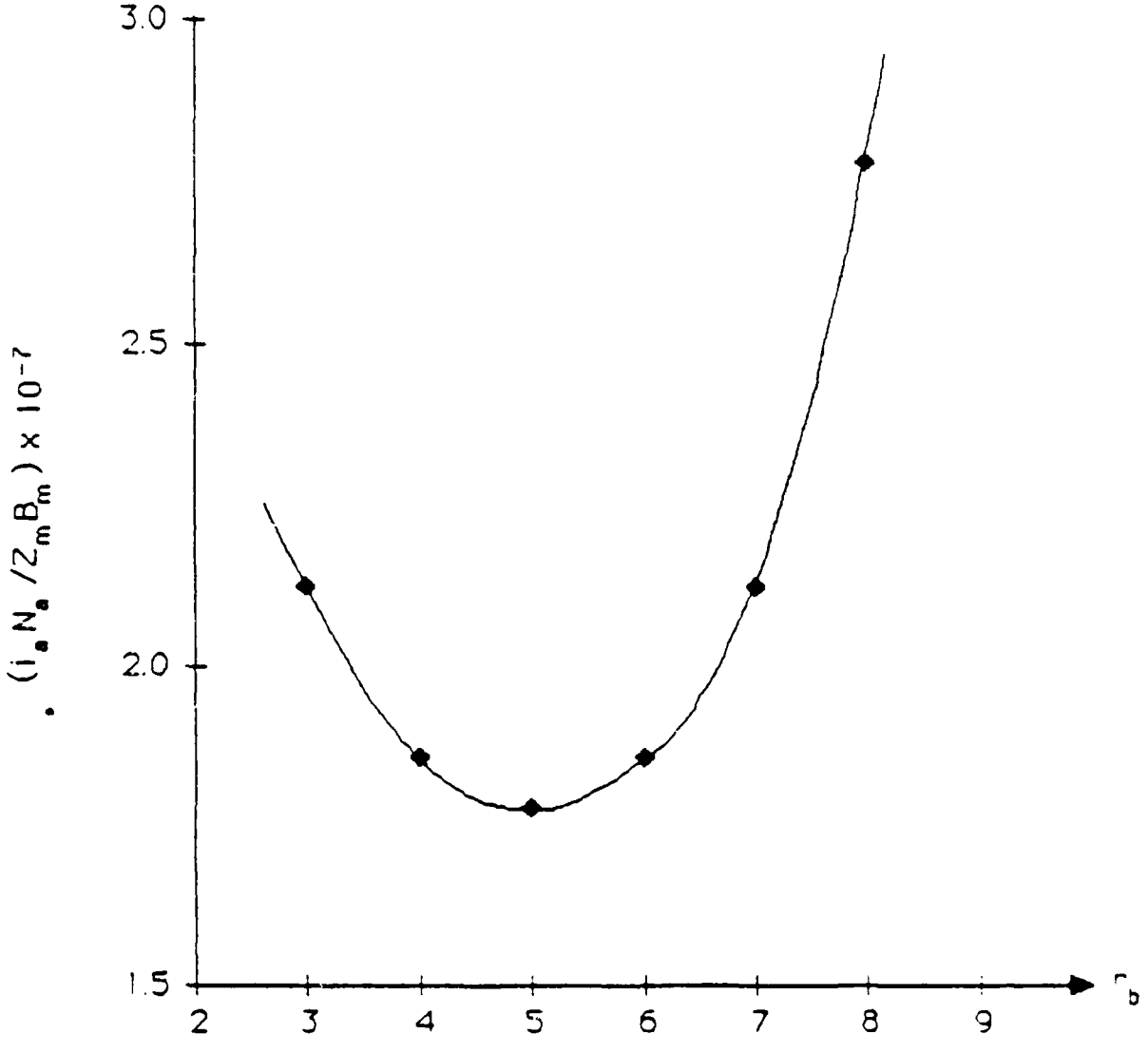

Figure VI—

Ampere-Turns (Coil A) Meter-Tesla
Versus B_b for B_a = 2 B_b

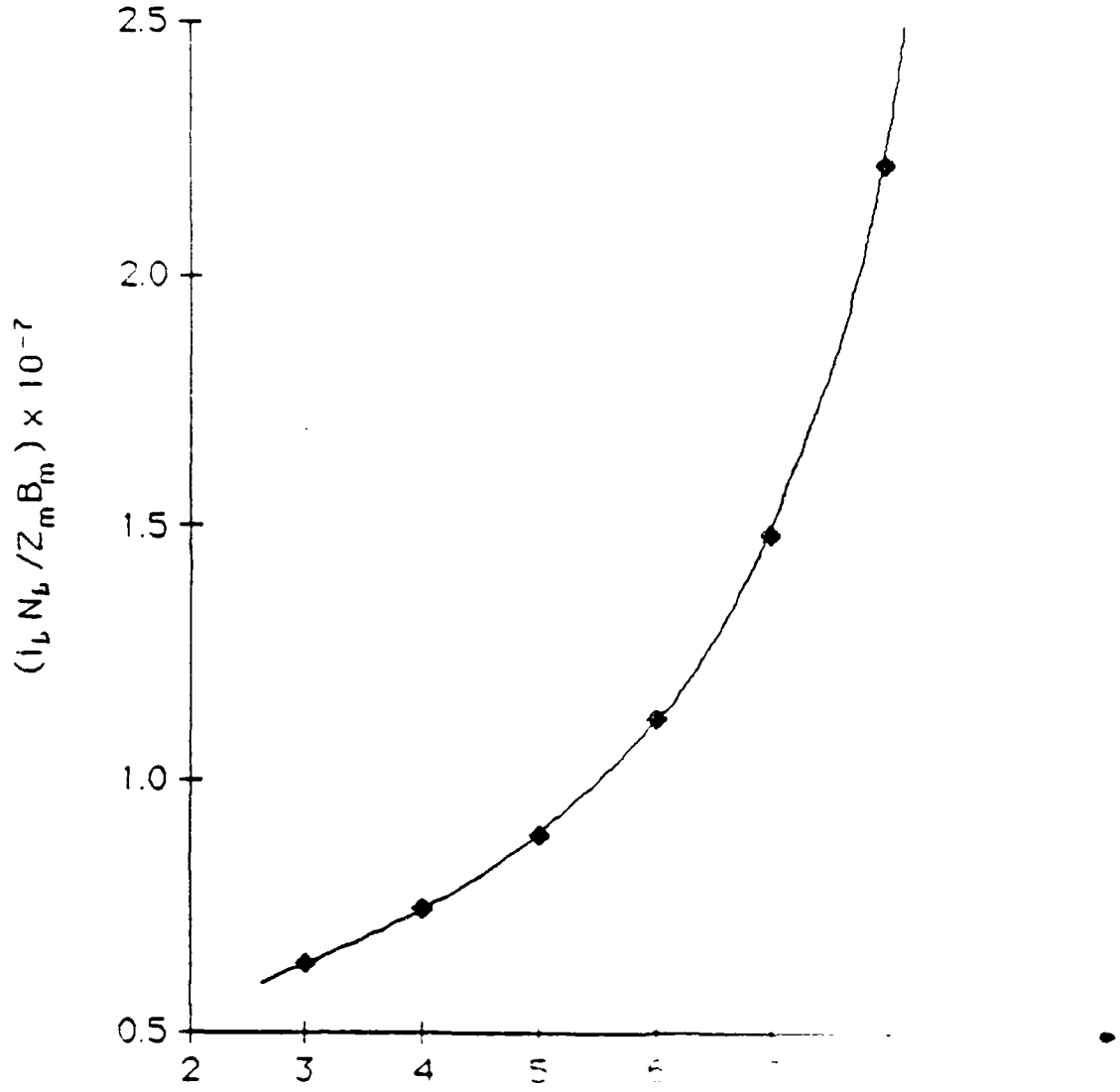
2.5
2.0
1.5
1.0
0.5
$(i_L N_L / Z_m B_m) \times 10^{-7}$
2
3
4
5

AD-A188169

UNCLASSIFIED

NAVAL OCEAN SYSTEMS CENTER, SAN DIEGO, CA
EVALUATION OF ONE-SIDED NUCLEAR MAGNETIC RESONANCE FOR REMOTE DETECTION OF EXPLOSIVES BY: LJ BURNETT, MA FINEMAN

2 OF 2
NOSC TD 1169
UNCLASSIFIED
OCT 1987

END
DATE
FILMED

Coil Geometries

The Inside-Out Helmholtz configuration offers a wide range of geometries suitable for single-sided NMR. This range is illustrated in the sketches of Figures VI-6 through VI-11.

These sketches, which are drawn to scale, show six separate Inside-Out Helmholtz geometries. The diameter of the outer coil is held constant in each of the sketches. The spheres on the Z-axis represent the relative sizes of the remote regions of field, with a 1% change in field representing the boundary.

It is obvious from this series of sketches that some coil geometries are more attractive than others for single-sided NMR. As the diameter of the inner coil increases, the distance to the remote region (i.e., the penetration depth) also increases. In addition, the size of the remote region increases. Therefore, those geometries with relatively large inner coil diameters would appear to be very attractive for single-sided NMR applications.

However, as the inner coil diameter increases, the figure-of-merit for the system decreases. This is a real effect and means that, all things being equal, a system with a smaller inner coil diameter will outperform one with a larger inner coil diameter.

There are two reasons for this result. First, the coupling between the remote region and the detector coil (and, hence, the figure-of-merit) varies as the inverse cube of the penetration depth. Second, the strength of the Ho field in the remote region decreases with increasing penetration depth.

The first effect is common to all remote NMR configurations and little can be done. Since there may be little advantage in operating the system at fields above about 1,000 Gauss, because of level crossing effects, the second effect may be partially compensated by choosing an attractive geometery and then increasing the current in the coils to produce the required external field. However, this strategy cannot be pursued indefinitely since the coils have current limits. These limits are discussed in the following section.

Coil Limitations

There are two potentially serious drawbacks to the use of superconducting coils in the proposed system. First, superconducting coils must be immersed in liquid helium. This problem would be very difficult to overcome were it not for a recent advance in cryogenic technology: the development of insulated containers that require refilling only three or four times a year and little maintenance. For a stationary field instrument, this should be adequate. For a portable system, though, the requirement for liquid helium may still pose serious problems.

Coil A	Coil B
$r_a = 10.0$	$r_b = 3.0$
$i_a = 1.0$	$i_b = 0.3$

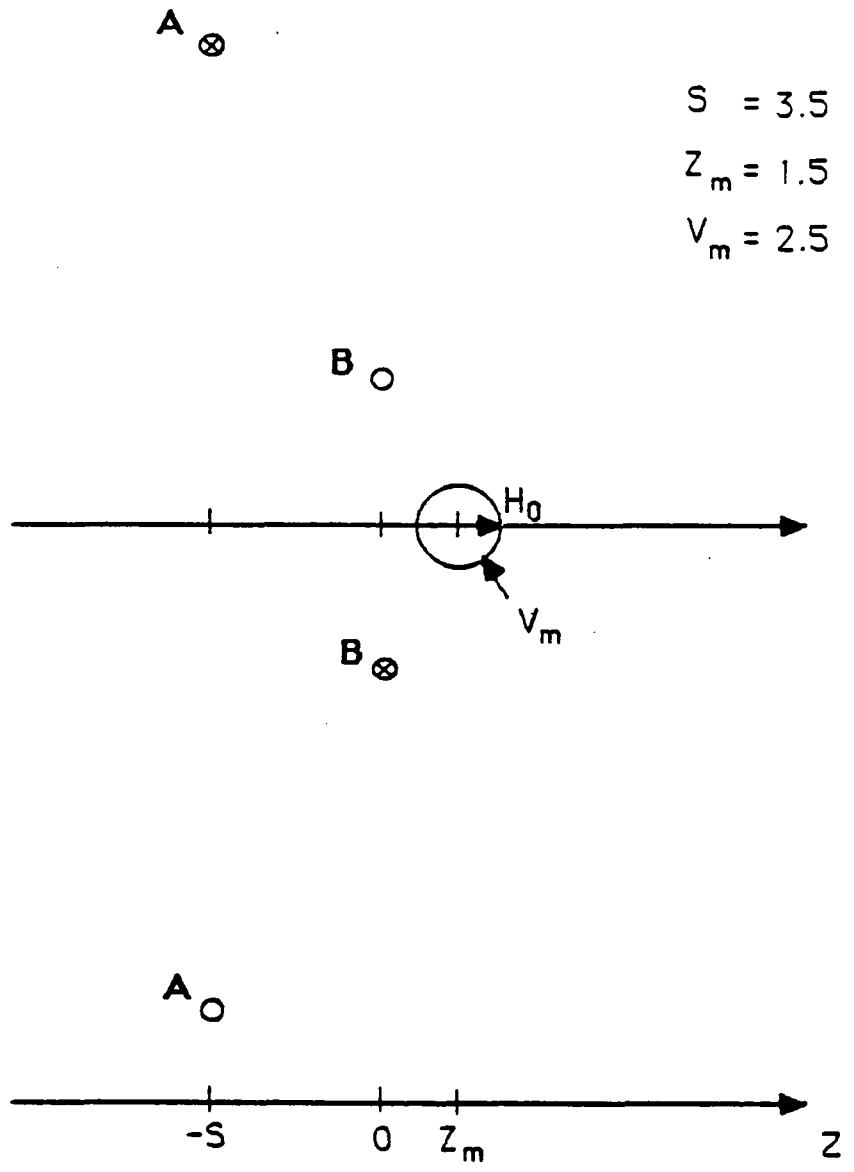

Figure VI-6

Inside-Out Helmholtz Geometry
For $R_a = 10$ and $R_b = 3$

Coil A	Coil B
$r_a = 10.0$	$r_b = 4.0$
$I_a = 1.0$	$I_b = 0.4$

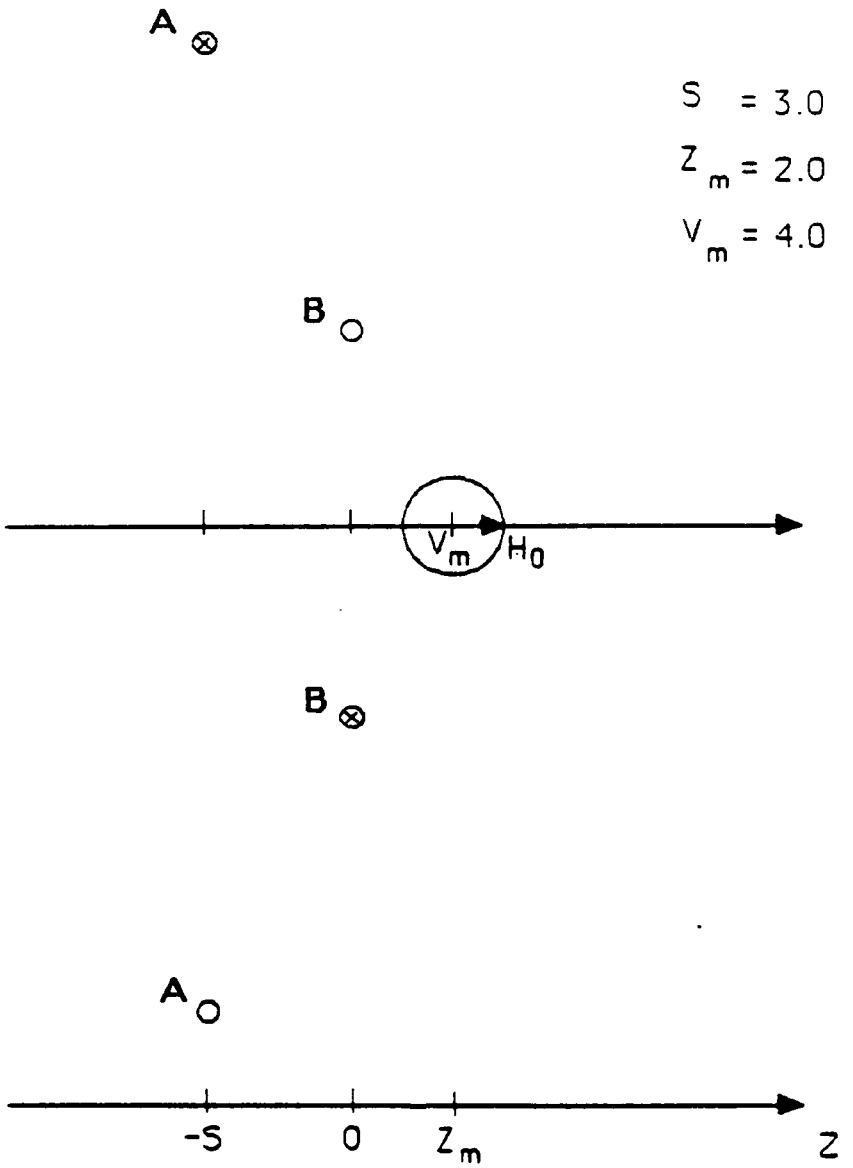

Figure VI-7

Inside-Out Helmholtz Geometry
For $R_a = 10$ and $R_b = 4$

Coil A	Coil B
$r_a = 10.0$	$r_b = 5.0$
$I_a = 1.0$	$I_b = 0.5$

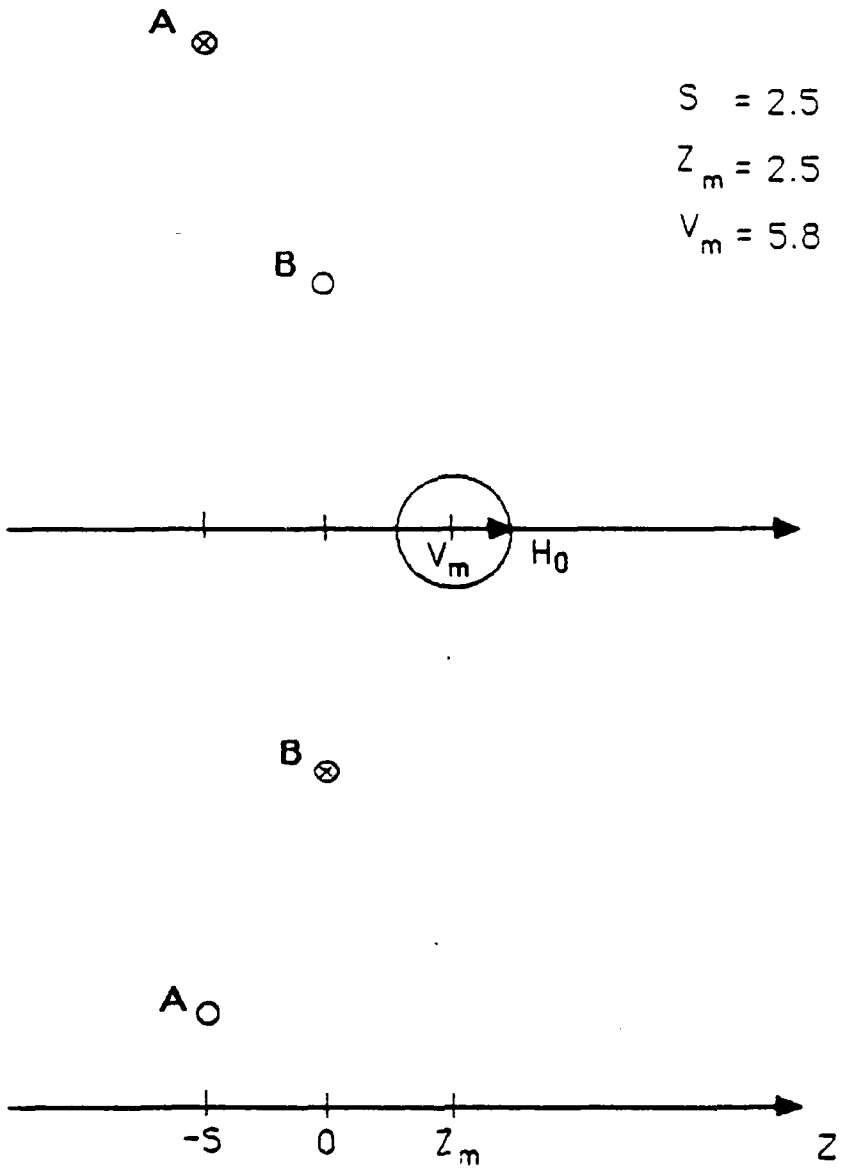

Figure VI-8

Inside-Out Helmholtz Geometry
For $R_a = 10$ and $R_b = 5$

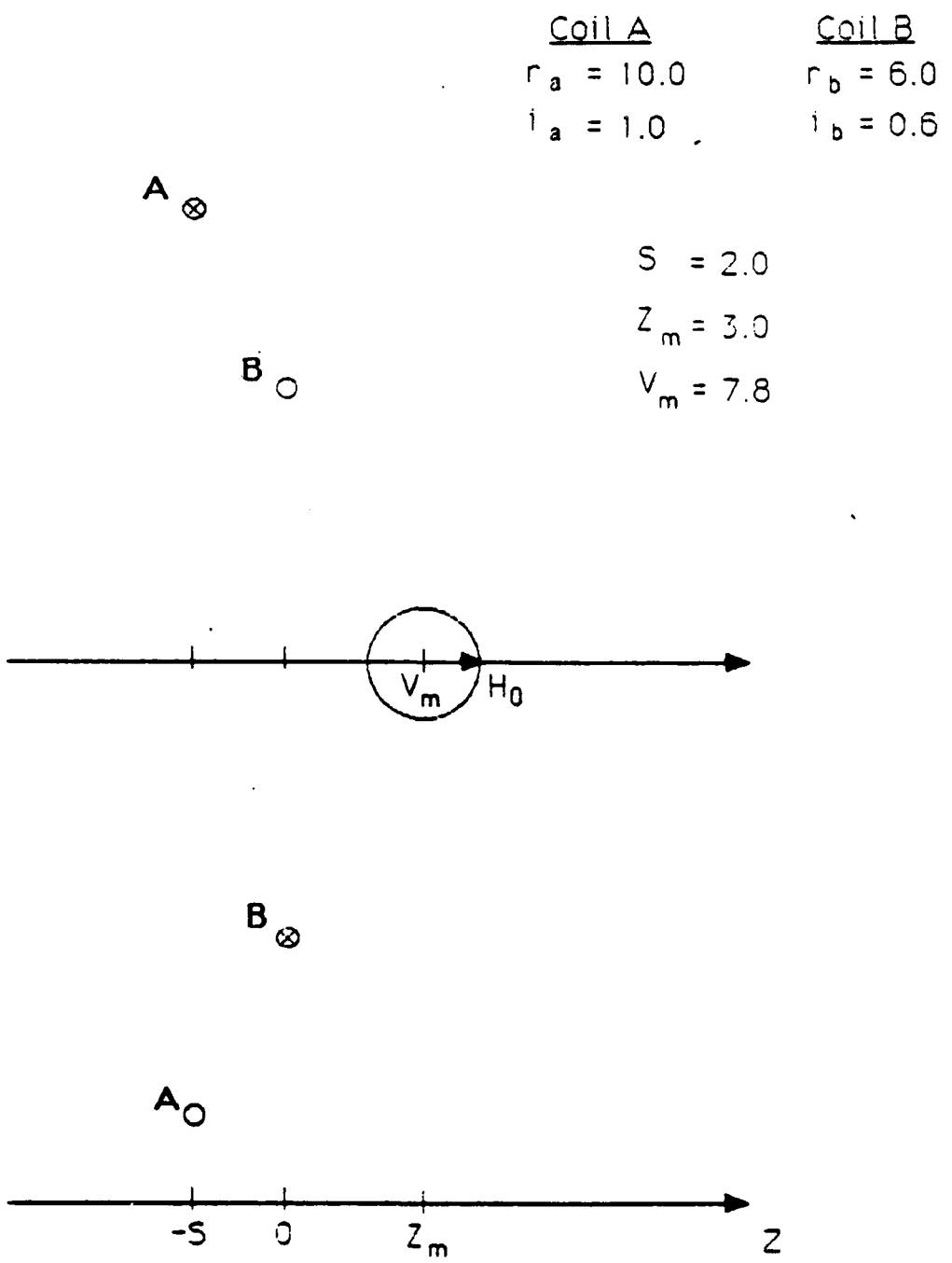

Figure VI-9

Inside-Out Helmholtz Geometry
For R_a = 10 and R_b = 6

Coil A	Coil B
$r_a = 10.0$	$r_b = 7.0$
$l_a = 1.0$	$l_b = 0.7$

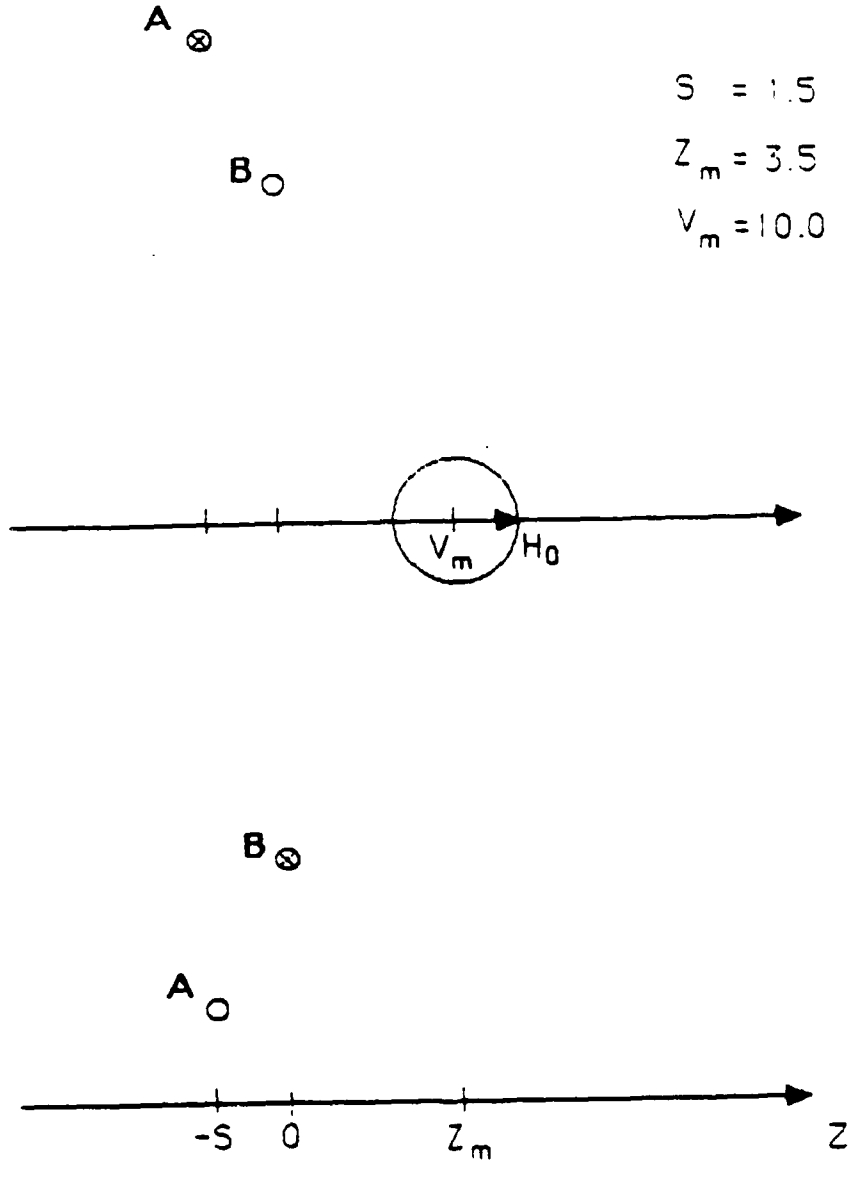

Figure VI-10

Inside-Out Helmholtz Geometry
For $R_a = 10$ and $R_b = 7$

Coil A	Coil B
$r_a = 10.0$	$r_b = 8.0$
$i_a = 1.0$	$i_b = 0.8$

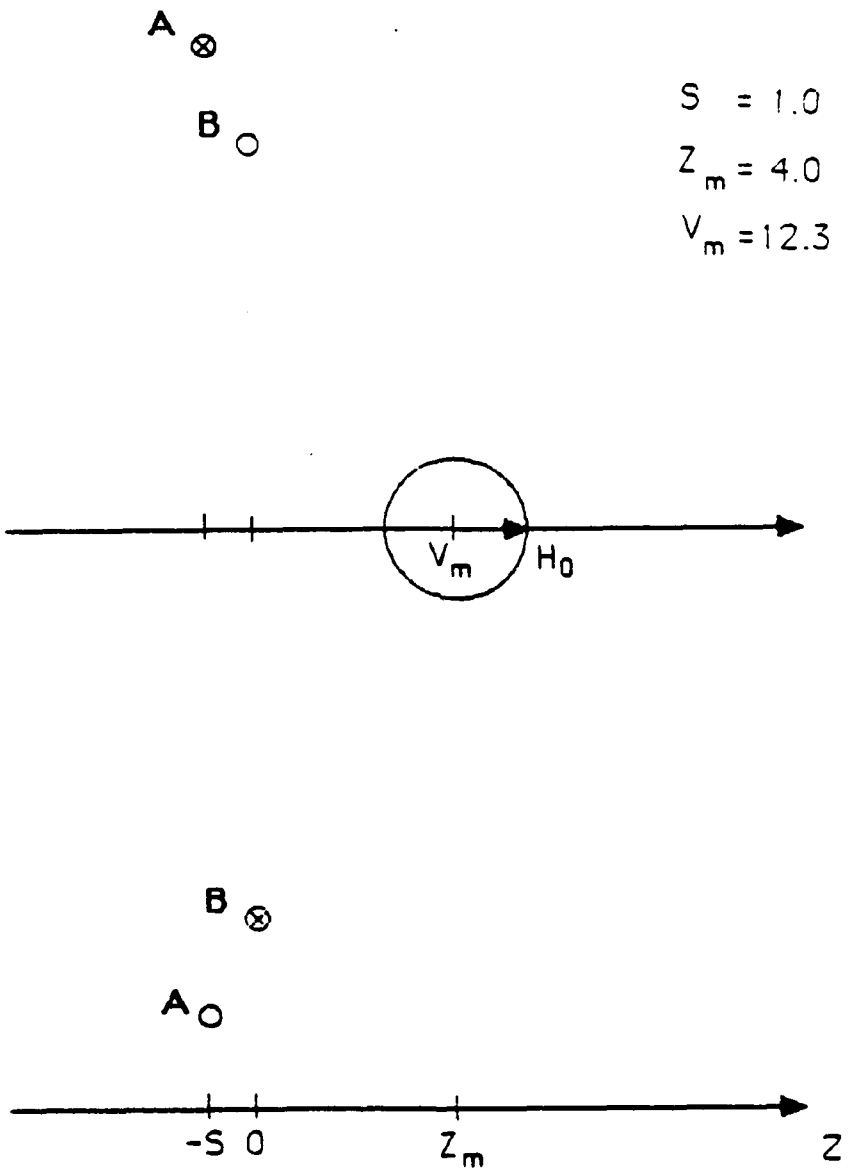

Figure VI-11

Inside-Out Helmholtz Geometry
For $R_a = 10$ and $R_b = 8$

Second, the maximum remote field attainable from a superconducting Inside-Out Helmholtz pair may not be adequate. The maximum field depends upon the maximum current that can flow through the coils, and the maximum current is determined by the magnitudes of the fields produced at the sites of the coil windings.

Superconducting materials can only tolerate magnetic fields up to a certain maximum before reverting to their normal state. The fields at the sites of the coils of an Inside-Out Helmholtz pair are determined by the configuration chosen and by the currents in the coils. The maximum remote field is reached when the limiting current is reached in one or both of the coils.

To address this problem, we contacted Dr. James Carolan, President of the Nalorac Cryogenics Corporation, a manufacturer of superconducting coils and associated components. Dr. Carolan analyzed this problem using a computer program developed for this purpose (26). His conclusions, for the Ra = 2(Rb) geometry, were that a 1,000 Gauss remote field with a penetration depth of 30 cm is certainly possible and that remote fields up to 2,000 Gauss may be achievable.

VII. CONCLUSIONS AND RECOMMENDATIONS

A. Conclusions

The results of this study lead to the following principal conclusions regarding remote detection of explosives using single-sided NMR technology.

1. Remote detection by single-sided NMR appears feasible. The present analysis indicates that useable penetration depths and adequate signal-to-noise ratios are attainable.

2. NMR remote detection of certain explosives is possible, but detailed data on the NMR properties of explosives are sparse. It may also be possible to define a unique signature, using hydrogen/nitrogen level crossing, for each explosive compound. Additional data and analyses are required.

3. An advanced NMR remote detection system will require superconducting coils to produce the magnetic field.

4. The preferred configuration will employ an Inside-Out Helmholtz pair to produce the magnetic field, and a semitoroid coil to produce the rf field.

B. Recommendations

These conclusions lead directly to the two recommendations presented below.

Recommendation 1. Acquire NMR data on the compounds of direct interest. Proton relaxation times and the effects of hydrogen/nitrogen interactions are of particular importance.

Recommendation 2. Perform a feasibility study for a field-useable system. Use the data from Recommendation 1, above, to address the possibility of discrimination between various explosives. Estimate inspection times under various sets of conditions.

VIII. NOMENCLATURE

Correlation Time. For random processes such as molecular motion, a measure of the time dependence of the fluctuations. In NMR, correlation times near the inverse of the Larmor frequency produce short T1 times.

Dead Time. The time for the NMR system to recover following an rf pulse, i.e., the time it takes for an FID to be visible after a pulse. Also called the recovery time.

FID. The NMR free induction decay signal following the application of an rf pulse, or pulses, at the Larmor frequency.

Free Induction Decay. See FID above.

Ho Field. The externally-applied magnetic field responsible for nuclear precession at the Larmor frequency.

H1 Field. The rf field applied at the Larmor frequency to tip the nuclear magnetization. The H1 field is applied perpendicular to the Ho field.

Inside-Out Helmholtz. A set of coils with spacing, radii and current flows arranged to produce a remote region of homogeneous field. At the remote field maximum, both the first and second derivatives of field strength with respect to distance are zero.

Inside-Out NMR. A particular type of remote NMR configuration in which opposed magnets are used to produce a toroidal remote region of homogeneous field. Originally developed for well logging applications.

Larmor frequency. The frequency at which the NMR experiment is performed; the precession frequency of the nuclei in the static magnetic field. The Larmor frequency is proportional to the strength of the static magnetic field and, for protons, is 4.26 MHz at 1,000 Gauss.

Polarization Time. The duration of time that the item to be inspected is immersed in the static magnetic field before interrogation by the NMR pulse sequence.

Recovery Time. See dead time above.

RF. Radio-frequency; in NMR, frequencies in the range of about 0.3 - 300 MHz.

RF Pulse. A short, intense burst of rf energy applied to the nuclei by the transmitter.

RF Pulse Sequence. A sequence of rf pulses designed to elicit a specific response from the nuclear spin system.

Solid Echo. A response from stongly coupled nuclei in solids produced by a sequence of two closely spaced rf pulses. The solid echo is often used to improve the SNR in systems while observing signals from short T2 materials.

SNR. The signal-to-noise ratio of the NMR system; usually refers to the voltage SNR.

Spin-Lattice Relaxation Time. See T1.

Spin-Spin Relaxation Time. See T2.

Static Field. See Ho field above.

T1. The spin-lattice relaxation time of the nuclear spin system. The characteristic time for the nuclear spin system to return to thermal equilibrium with its surroundings following a disturbance.

T2. The spin-spin relaxation time of the nuclear spin system. The characteristic time for the nuclear spin system to return to internal equilibrium following a disturbance.

XI. REFERENCES

1. L. J. Burnett, "A Study To Review and Evaluate Customs Nuclear Magnetic Resonance Equipment and Programs", Final Report on U.S. Customs Contract TC 84-25, January 1985.

2. J. D. King, W. L. Rollwitz, and G. A. Matzkanin, "Nuclear Magnetic Resonance Techniques for Explosives Detection", U.S. Army, Final Report on Contract Number DAAK02-74-C-0056, June 1975.

3. G. A. Matzkanin, A. DeLosSantos, and D. A. Whiting, "Determination of Moisture Levels in Structural Concrete Using Pulsed NMR", U.S. Department of Transportation, Final Report on Contract Number DOT-FH-11-9487, April 1982.

4. G. A. Matzkanin and A. DeLosSantos, "In-Situ Determination of Moisture Levels in Structural Concrete by a Modified NMR Method", U.S. Department of Transportation, Final Report on Contract Number DTFH61-83-C-00015, May 1985.

5. R. K. Cooper and J. A. Jackson, "Remote (Inside-Out) NMR I. Remote Production of a Region of Homogeneous Magnetic Field" Journal of Magnetic Resonance 41, 400 (1980).

6. L. J. Burnett and J. A. Jackson, "Remote (Inside-Out) NMR II. Sensitivity of NMR Detection for External Samples", Journal of Magnetic Resonance 41, 406 (1980).

7. J. A. Jackson, L. J. Burnett and J. F. Harmon, "Remote (Inside-Out) NMR III. Detection of Nuclear Magnetic Resonance in a Remotely-Produced Region of Homogeneous Magnetic Field", Journal of Magnetic Resonance 41, 411 (1980).

8. E. R. Andrew, Nuclear Magnetic Resonance, Cambridge University Press, Cambridge, 1955.

9. A. Abragam, The Principles of Nuclear Magnetism, Clarendon Press, Oxford, 1961.

10. T. C. Farrar and E. D. Becker, Pulse and Fourier Transform NMR; Introduction to Theory and Methods, Academic Press, New York, 1971.

11. E. Fukushima and S. B. W. Roeder, Experimental Pulse NMR, A Nuts and Bolts Approach, Addison-Wesley, Reading, MA, 1981; pages 463-7.

12. Reference 3, page 39 (as corrected).

13. D. I. Hoult and R. E. Richards, "The Signal-to-Noise Ratio of the NMR Experiment", Journal of Magnetic Resonance 24, 71 (1976).

14. C. L. Hutchinson, ed., The ARRL Handbook for the Radio Amateur, American Radio Relay League, Newington, CT, 1985.

15. R. E. Richards, "The Principles Involved in the Study of Molecular Motion in Solids by NMR", a chapter in Molecular Dynamics and Structure of Solids, R. S. Carter and J. J. Rush, eds., NBS Special Publication 301, June 1969.

16. E. R. Andrew, "NMR and Molecular Motion in Organic Crystals", a chapter in Molecular Dynamics and Structure of Solids, R. S. Carter and J. J. Rush, eds., NBS Special Publication 301, June 1969.

17. C. Baker, "Proton Relaxation and Molecular Motion in Polyisobutylene", M.S. Thesis, San Diego State University, August 1986.

18. B. M. Dobratz, ed., LLNL Explosives Handbook -- Properties of Chemical Explosives and Explosives Simulants, University of California Technical Report, UCRL-52997 (1981).

19. R. T. Barbour, Pyrotechnics In Industry, McGraw-Hill, New York,

20. T. Urbanski, Chemistry and Technology of Explosives, M. Jurecki, ed., S. Laverton, transl., Pergamon, Oxford,

21. A. N. Garroway and H. A. Resing, "Proton Relaxation in 1,3,5-Triamino-2,4,6-Trinitrobenzene (TATB)", Naval Research Laboratory Memorandum Report 4250, June 1980.

22. L. J. Burnett, "A Study To Evaluate Nuclear Magnetic Resonance For Narcotics Detection", Final Report on U.S. Customs Contract CS-085-2075-1, April 1986.

23. A. R. Rath, S. B. W. Roeder, and E. Fukushima, "Opposed Coil Magnet Calculations For Large Sample and Unilateral Nuclear Magnetic Resonance", Review of Scientific Instruments 56, 402 (1985).

24. E. Fukushima, S. B. W. Roeder, R. A. Assink, and A. A. V. Gibson, "Nuclear Magnetic Resonance Apparatus Having Semi-toroidal RF Coil For Use In Topical NMR And NMR Imaging", U.S. Patent Number 4,590,427; May 1986.

25. J. A. Brown, J. A. Jackson, and A. R. Koelle, "Western Gas Sands Project Los Alamos NMR Well Logging Tool Development", Los Alamos National Laboratory Report Number LA-10374-PR, March 1985.

26. Dr. James L. Carolan, Nalorac Cryogenics Corporation, 837 Arnold Drive, Suite 600, Martinez, California, 94553; private communication.

END
DATE
FILMED

12-8-87